Characteristics of Endoplasmic Reticulum-derived Transport Vesicles

Michael F. Rexach, Martin Latterich, and Randy W. Schekman

Department of Molecular and Cell Biology and Howard Hughes Medical Research Institute, University of California, Berkeley, Berkeley, California 94720

Abstract. We have isolated vesicles that mediate protein transport from the ER to Golgi membranes in perforated yeast. These vesicles, which form de novo during in vitro incubations, carry lumenal and membrane proteins that include core-glycosylated pro-α-factor, Bet1, Sec22, and Bos1, but not ER-resident Kar2 or Sec61 proteins. Thus, lumenal and membrane proteins in the ER are sorted prior to transport vesicle scission. Inhibition of Ypt1p-function, which prevents newly formed vesicles from docking to *cis*-Golgi membranes, was used to block transport. Vesicles that accumulate are competent for fusion with *cis*-Golgi membranes, but not with ER membranes, and thus are functionally committed to vectorial transport. A 900-fold enrichment was developed using differential centrifugation and a series of velocity and equilibrium density gradients. Electron microscopic analysis shows a uniform population of 60 nm vesicles that lack peripheral protein coats. Quantitative Western blot analysis indicates that protein markers of cytosol and cellular membranes are depleted throughout the purification, whereas the synaptobrevin-like Bet1, Sec22, and Bos1 proteins are highly enriched. Uncoated ER-derived transport vesicles (ERV) contain twelve major proteins that associate tightly with the membrane. The ERV proteins may represent abundant cargo and additional targeting molecules.

MORPHOLOGICAL analysis of eukaryotic cells led to the hypothesis that small vesicles mediate the directional transport of proteins between successive organelles of the secretory pathway (Jamieson and Palade, 1967; Palade, 1975). The machinery that catalyzes vesicular transport is now being studied at the molecular level using in vitro assays that reconstitute intercompartmental protein transport in perforated cells and membrane extracts (Pryer et al., 1992). The characterization of vesicles that mediate intercompartmental protein transport in vitro will help address the role of integral membrane proteins that function in vesicular traffic.

Although most transport vesicles are transient intermediates, they can be forced to accumulate as stable intermediates when a component of the vesicle targeting machinery is inactivated. Most transport vesicles are 50–100 nm in size and may be coated with a peripheral protein lattice. In coated transport vesicles, the subunits of the coat are the most abundant proteins in pure vesicle preparations. Clathrin complexes coat vesicles derived from the *trans*-Golgi and plasma membranes (Brodsky, 1988). Assembly of clathrin lattices onto the donor membrane is guided by adaptins and ADP ribosylation factor (ARF)[1] proteins, and functions to select a cargo of membrane proteins, and to drive vesicle budding (Pearse and Robinson, 1990; Keen, 1990; Stamnes et al., 1993). On the other hand, nonclathrin coatomer complexes coat vesicles derived from Golgi membranes (Malhotra et al., 1989). Assembly of coatomer onto membranes is guided by ARF and functions to drive the membrane shape change that accompanies budding (Palmer et al., 1993; Orci et al., 1993). In both cases, coats disassemble prior to vesicle fusion with the target membrane (Brodsky, 1988; Orci et al., 1989). Most proteins in uncoated transport vesicles are tightly associated with the membrane. For example, uncoated synaptic vesicles contain various integral membrane proteins with distinct structural features; the most abundant are termed synaptobrevin, synaptophysin, and synaptotagmin (Südhof and Jahn, 1991). These membrane proteins are thought to promote vesicle targeting or fusion to the plasma membrane.

Insight into the components and mechanics of vesicle-mediated protein transport has been provided by genetic analysis of the yeast *Saccharomyces cerevisiae.* More than 25

M. F. Rexach's present address is Laboratory of Cell Biology, Box 168, The Rockefeller University, New York, NY 10021.

Address all correspondence to R. W. Schekman, Department of Molecular and Cell Biology and Howard Hughes Medical Research Institute, University of California, Berkeley, Berkeley, CA 94720.

1. *Abbreviations used in this paper*: ARF, ADP ribosylation factor; CPK, creatine phosphokinase; F, Ficoll; core-gpαf, core-glycosylated pro-α-factor; MSS, medium speed supernatant fraction; pαf, pro-α-factor; ppαf, pre-pro-α-factor; s, sucrose.

proteins that play essential roles in ER to Golgi protein transport have been identified (Pryer et al., 1992) and their function tested using temperature-sensitive mutants, or by depleting cells of the protein in question. Cells that contain a mutant form of Sec12, Sec13, Sec16, or Sec23 proteins are blocked in ER to Golgi protein transport and accumulate enlarged ER membranes (Novick et al., 1980; Novick et al., 1981; Kaiser and Schekman, 1990). These proteins are thought to function in the formation of ER-derived transport vesicles. In contrast, cells that contain a mutant form of Ypt1, Sec22, Sec18, or Sec17, and cells depleted of Bos1 or Sed5 proteins are deficient in protein transport from ER to the Golgi membranes and accumulate 50–60 nm vesicles and enlarged ER membranes (Kaiser and Schekman, 1990; Shim et al., 1991; Becker et al., 1991; Hardwick and Pelham, 1992). Because these cells accumulate small vesicles, these proteins are thought to function in the targeting or fusion of ER-derived transport vesicles.

The function of proteins identified in genetic screens can be tested directly using in vitro assays that reconstitute ER to Golgi protein transport in perforated yeast spheroplasts or microsomal preparations (Baker et al., 1988; Ruohola et al., 1988). Subassays that measure vesicle budding, targeting, and fusion have allowed a direct assessment of the protein, nucleotide, and ionic requirements for each stage (Rexach and Schekman, 1991). The release of vesicles from ER membranes requires GTP and the function of Sec12p, Sar1p, Sec23/24p complex, and Sec13/31p complex (Rexach and Schekman, 1991; Oka and Nakano, 1991; d'Enfert et al., 1991; Hicke et al., 1992; Barlowe et al., 1993*a*,*b*; Pryer et al., 1993; Salama et al., 1993). The stable attachment of transport vesicles to Golgi membranes requires the function of Ypt1 and Sec18 proteins, whereas fusion between vesicle and the *cis*-Golgi membranes requires calcium and ATP at physiological temperature (Rexach and Schekman, 1991). Specific antibodies against Sec7p and Bos1p block vesicle targeting or fusion (Franzusoff et al., 1992; Lian and Ferro-Novick, 1993).

Here we report the purification of ER-derived transport vesicles that accumulate in vitro when perforated yeast cells of a Ypt1p-deficient strain are incubated with cytosol and an ATP regeneration system at physiological temperature. We examined the function and molecular composition of purified transport vesicles, and provide a direct biochemical demonstration that diffusible vesicles mediate selective and vectorial transport of lumenal and membrane proteins from the endoplasmic reticulum to the Golgi complex.

Materials and Methods

The yeast strains used in this study were RSY 445 (*leu 2-3,112*; *ura 3-52*; *trp1-289*; *prb1*, *pep4*::*URA3*; *gal2*; *his 4-579*; *MAT*α), RSY 607 (*ura3-52*; *leu2-3,112*; *pep4*::*URA3*; *MAT*α), RSY 453 (*ypt1*^{ts}:*LEU2*, *gls1-1*; *leu2*; *his3*, *ura3-52*; *MAT*α), RSY 1001 (*ypt1*^{ts}:*LEU2*; *gls1-1*; *leu2*; *his3*; *ura3-52*; *pep4*::*URA3*; *MAT*α) and MLY 1601 *ypt1*^{ts}::*LEU2* (*gls1-1*, *leu2-3,112*, *ura3-52*, *pep4*::*URA3*).

Preparation of Perforated Yeast Spheroplasts

Cells were grown at 30°C (wild-type) or 24°C (*ypt1* ts) in YP medium (1% Bacto yeast extract, 2% Bacto peptone; Difco Laboratories Inc., Detroit, MI), and 5% glucose to early log phase (2–4 OD_{600}/ml; 1 OD U is 10^7 cells). Approximately 2,000 OD_{600} cells were harvested by centrifugation at 5,000 rpm for 5 min in a GSA Sorvall rotor chilled to 4°C. Cells were resuspended to 50 OD_{600}/ml in 10 mM Tris, pH 9.4, 10 mM DTT and incubated for 5 min at room temperature. Cells were sedimented at 2,000 *g* for 5 min at room temperature in a clinical centrifuge and resuspended to 50 OD_{600}/ml in spheroplasting medium (0.75× YP, 0.7 M sorbitol, 0.5% glucose, 10 mM Tris, pH 7.5). The initial integrity of the cell wall was determined by diluting an aliquot of cells 1:100 in water, and measuring the OD_{600} after 1 min. Lyticase was mixed with the cells (30 U/OD_{600} for wild-type, and 60 U/OD_{600} for *ypt1* ts) and incubated at 24°C (*ypt1* ts) or 30°C (wild-type) until the OD_{600} readings of cell aliquots were less than 10% of the initial OD_{600} value. Spheroplasts were sedimented at 2,000 *g* for 5 min as before, resuspended to 5 OD_{600}/ml in regeneration medium (0.75× YP, 0.7 M sorbitol, 1% glucose), and incubated with gentle shaking during 30 min at 24°C (*ypt1* ts) or 30°C (wild-type). Spheroplasts were harvested by centrifugation at 5,000 rpm for 5 min at 4°C in a Sorvall GSA rotor, and resuspended to 100 OD_{600}/ml in lysis buffer (20 mM Hepes, pH 6.8, 400 mM sorbitol, 150 mM KOAc, 2 mM MgOAc, 0.5 mM EGTA). Cells were transferred to a 40 ml Sorvall ultracentrifuge tube and sedimented at 6,000 *g* for 5 min at 4°C in a Sorvall SS34 rotor. For small-scale perforated cell preparations, we resuspended spheroplasts to 300 OD_{600}/ml in lysis buffer, aliquoted them in 200 μl portions into 1.5 ml microcentrifuge tubes, and froze them by suspension over liquid nitrogen vapor for 30 min (see Baker et al., 1989). For large-scale perforated cell preparations, we resuspended spheroplasts to 100 OD_{600}/ml, sedimented them as before, and froze them as a cell pellet by storing at −70°C. After thawing, spheroplasts were perforated using low osmotic support buffer (see below).

Preparation of Membrane-free Cytosol

Cells were grown at 24°C (*ypt1* ts) or 30°C (wild-type) in YP medium, 5% glucose to log phase (5–10 OD_{600}/ml), and ~6,000 OD_{600} cell units were harvested by centrifugation at 5,000 rpm for 5 min at 4°C in a Sorvall GSA rotor. All subsequent steps were carried out at 4°C. Cells were resuspended in 60 ml distilled water and washed twice by sedimentation at 6,000 *g* for 5 min and dilution in distilled water. Cell pellets were frozen at −70°C. Thawed cell pellets were washed once with B88 (20 mM Hepes, pH 6.8, 150 mM KOAc, 250 mM sorbitol, 5 mM MgOAc), resuspended in 60 ml of B88, and 20 ml portions (2,000 OD_{600} U) aliquoted into Corex 30 ml glass tubes. Cells were sedimented as before and to each tube, 4 g of glass beads (0.5-mm diam) and 1 ml of solution A (20 mM Hepes, pH 6.8, 50 mM KOAc, 100 mM sorbitol, 5 mM MgOAc, 1 mM ATP, 0.5 mM PMSF, 1 mM DTT) were added. Cells were lysed by 6 × 30 s periods of agitation in a VWR vortexer (Scientific Industries, Inc., Bohemia, NY) at full speed, with 1-min incubations on ice in between periods. To each sample, 1.5 ml of solution B (20 mM Hepes, pH 6.8, 2 M KCl, 400 mM sorbitol, 5 mM MgOAc, 1 mM ATP, 0.5 mM PMSF, 1 mM DTT) was added and tubes were vortexed 3 × 30 s at full speed. The homogenate was clarified by centrifugation at 12,000 *g* for 5 min in a Sorvall SS34 rotor. The combined supernatants (9 ml) were mixed with an equal volume of 80% Nycodenz, 20 mM Hepes, pH 6.8, 150 mM KOAc, 5 mM MgOAc, and transferred into two 11.5 ml Ultraclear tubes (Beckman Instruments, Palo Alto, CA) and overlaid with 2.5 ml 20 mM Hepes, pH 6.8, 150 mM KOAc, 5 mM MgOAc. The tubes were centrifuged for 21 h at 35,000 rpm in a SW41 Beckman rotor. Cytosol (7.5 ml) was slowly drained from the bottom of each tube, avoiding the membranes and lipid particles that accumulate in the 40%/0% Nycodenz interface. The cytosol pool (15 ml) was applied to the bottom of a top-fitted Sephadex medium G-25 desalting column (80 ml packed resin) equilibrated in B88, 1 mM ATP. The sample was pumped upwards at a flow rate of 1 ml/min using a Rainin Rabbit pump (Woburn, MA), and fractions collected from the top. The eluted protein peak was pooled, aliquoted, frozen in liquid nitrogen, and stored at −70°C. Protein concentration was usually 9 mg/ml, and was measured by the Bradford protein assay and compared to a BSA standard.

In Vitro Transport

Reagents used for the in vitro transport assay were obtained as described in Baker et al. (1988, 1989) unless otherwise indicated.

Stage I: Translocation. For each experiment a frozen aliquot of perforated yeast spheroplasts (Fig. 60 OD_{600} U of cell equivalents) was thawed and washed once by dilution in B88 and sedimented at 13,000 *g* for 40 s in a refrigerated microcentrifuge (Tomy Tech USA Inc., Palo Alto, CA). The cell pellet was resuspended in 1 ml low osmotic support B88 (20 mM Hepes, pH 6.8, 50 mM KOAc, 250 mM sorbitol, 5 mM MgOAc) to maximize spheroplast lysis (>90% perforated). After 1 min at 4°C, membranes were sedimented, washed once with B88 as before, and resuspended in 0.1 ml of a yeast S-100 translation lysate that contained [^{35}S]methionine-

prepro-α-factor (ppαf), plus 16 μl of a 10× ATP regeneration mix (Baker et al., 1988) in final volumes of 160 μl. The final concentration of components in a 25-μl translocation reaction was 75 μg of membranes (measured by the amido-black protein assay described in the Materials and Methods), 90 μg of yeast S100 lysate (measured by the Bradford protein assay), 50 μM GDP-mannose, 1 mM ATP, 40 mM creatine phosphate (CP), and 200 μg/ml creatine phosphokinase (CPK), all dissolved in B88. The mix was incubated 15 min at 10°C to allow posttranslational translocation of ppαf, chilled to 4°C, diluted with 1 ml B88, and sedimented as before. Membranes were resuspended in 1 ml of high-salt B88 (20 mM Hepes, pH 6.8, 1 M KOAc, 250 mM sorbitol, 5 mM MgOAc) and rotated at 4°C for 7 min. Membranes were sedimented, washed once with B88 and the final membrane pellet resuspended to 160 μl (30 μg/10 μl).

Stage II: Transport. Each transport reaction (25 μl) contained 10 μl of stage I membranes, 90 μg of membrane-free cytosol, 1 mM ATP, 50 μM GDP mannose, 40 mM CP, 200 μg/ml CPK, in B88. For time courses, a 200 μl stage II mix was prepared and aliquoted in 25-μl portions into 0.5 ml microcentrifuge tubes. Reactions were incubated at 0° or 25°C for the indicated times, each tube represented one time point. Reactions were terminated by placing each tube on ice until the last time point was taken. Aliquots (15 μl) of each time point were treated with 10 μl of a trypsin solution (625 μg/ml in B88) for 10 min on ice, and then with 10 μl of a trypsin inhibitor solution (1.25 mg/ml in B88), for 10 min on ice. Each sample received 45 μl of 2× Laemmli sample buffer without reducing agent, and was heated at 95°C for 10 min. Equal aliquots of each tube were treated with either Con A–Sepharose, or protein A–Sepharose coupled with anti-α1,6 antibody as described by Baker et al. (1988). Washed immunoprecipitates were heated to 95°C in 1% SDS for 5 min and dissolved in Universol ES scintillation fluid (ICN Biomedicals, Irvine, CA) for quantitation in a scintillation counter. Glycosylated forms of α-factor are the major radiolabeled proteins.

Stage III: Transport Vesicle Chases. Aliquots (5 μl) of purified transport vesicles or pool 1 fractions were mixed with membrane-free cytosol, perforated wild-type yeast spheroplasts or microsomes, and an ATP regeneration system, to the same concentrations as for stage II of transport (see above) in a total volume of 50 μl. Chases were conducted for 1 h at 0° or 20°C in the presence of various additions (i.e., cytosol, membranes, ATP). Reactions were terminated by the addition of 50 μl of 2× Laemmli sample buffer without reducing agent, and were processed for their content of gpαf as described for stage II transport.

Vesicle Budding and Fusion Assay

Stage II transport reactions were terminated by placing tubes on ice (see above), and each tube was fractionated by centrifugation for 40 s at 13,000 rpm in a refrigerated microcentrifuge (Tomy Tech USA Inc.). A 15-μl medium speed supernatant fraction (MSS) was taken from the meniscus and treated with trypsin and trypsin inhibitor, then mixed with Laemmli sample buffer without reducing agent, and aliquots processed for Con A and α1,6 antibody precipitation as for stage II transport. A 15-μl aliquot of unfractionated reactions is referred to as total, and served to calculate the "% released" of protein markers from perforated cells. Budding efficiency is expressed as the percentage of protease protected gpαf/μl of the MSS fraction over protease protected gpαf/μl of the total fraction.

ER-Protein Sorting Assay

To measure the release or retention of lumenal ER-proteins, vesicle budding assays were performed as described above, with 2% beta-mercaptoethanol (β-ME) included in the Laemmli sample buffer. To measure the release or retention of membrane embedded ER-proteins, vesicle budding assays were performed in the absence of radiolabeled [^{35}S]-pro-α-factor (an S100 translation lysate without radiolabeled pre-pro-α-factor was used for Stage I). After samples were fractionated in a microcentrifuge, they were mixed with 25 μl of 2× Laemmli buffer with 2% β-ME, and heated at 65°C for 15 min. Aliquots (15 μl) were subjected to SDS-PAGE in 14% acrylamide mini-gels, and [^{125}I]-Protein A western blots were performed as described below.

ER-Membrane Fusion Assay

Aliquots (5 μl) of an enriched transport vesicle preparation (from pool 1) were mixed with 100 μg of wild-type membrane-free cytosol, 25 μg of wild-type yeast microsomes (prepared as in Wuestehube and Schekman, 1992), and an ATP regeneration system, in a total volume of 50 μl. Chases were conducted for 1 h at 0° or 20°C in the presence of various additions (i.e., GDP-mannose, cytosol, Triton X-100). Chilled reactions were treated with trypsin and then trypsin inhibitor (as for stage II transport) to degrade gpαf that was not membrane enclosed. Reactions were terminated by the addition of 60 μl of 2× Laemmli sample buffer without reducing agent and samples were processed for their content of gpαf as described for stage II transport, or mixed with 2% β-ME and resolved in a 12.5% SDS-PAGE. Gels were fixed, dried, and exposed to phosphor plates. The percentage of glucose trimming (i.e., the conversion of the 32-kD *glsl*-1 form of core-gpαf to the 29-kD wild-type form) was quantified using standard software in a Molecular Dynamics PhosphorImager (Sunnyvale, CA). For a more detailed description of the ER-membrane fusion assay see Latterich and Schekman (1994).

Vesicle-targeting/Docking Assay

Membranes released from perforated cells during stage II incubations were subjected to velocity sedimentation in a Ficoll (F)/sucrose (s) gradient that resolves diffusible vesicles from *cis*-Golgi membranes. Stage II reactions (400 μl) were incubated 35 min at 25°C and then chilled. MSS fractions (300 μl) were obtained after sedimenting perforated cells at 13,000 *g* for 90 s at 4°C. Each MSS fraction was loaded into a 5 ml Beckman Ultraclear tube that contained 600 μl of 60% s (wt/vol)/5% F (wt/vol) at the bottom, layered with 1 ml of 4% F/15% s, 1 ml 3% F/15% s, 1 ml 2% F/15% s, and 1 ml 1% F/15% s all dissolved in reaction buffer without sorbitol. Tubes were centrifuged 2 h at 35,000 rpm in a Beckman SW 50.1 ultracentrifuge rotor. 18 aliquots (300 μl) were collected from the top using a gradient collector (Isco Inc., Lincoln, NE). Fractions were analyzed for their content of GDPase activity, refractive index, and content of radioactive gpαf.

Vesicle Purification

A pellet of frozen yeast spheroplasts (2,000 OD_{600} U of cell equivalents; see preparation of perforated yeast spheroplasts) was thawed, and washed once by dilution in chilled B88. Spheroplasts were sedimented at 12,000 *g* for 2 min at 4°C in a Sorvall SS34 rotor, and the pellet (1 ml) was resuspended in 2 ml of B88. The sample was mixed with 15 ml of low osmotic support B88 (20 mM Hepes, pH 6.8, 50 mM KOAc, 250 mM sorbitol, 5 mM MgOAc), and allowed to stand at 4°C for 1 min to allow spheroplast lysis; lysis was stopped by mixing the sample with 2 ml of high-salt B88 (20 mM Hepes, pH 6.8, 1 M KOAc, 250 mM sorbitol, 5 mM MgOAc). Perforated cells were washed with B88, the pellet was resuspended in 1 ml of B88, and the cell suspension was mixed with 1–3 ml of a yeast S-100 translation lysate that contained [^{35}S]methionine-ppαf, and with 0.4 to 0.6 ml of a 10× ATP regeneration mix (Baker et al., 1988) in final volumes of 4 to 6 ml. The mix was incubated for 20 min at 10°C to allow posttranslational translocation (stage I), and chilled for 10 min at 4°C. The sample was diluted to 15 ml with B88, sedimented as before, and membranes resuspended in 10 ml of high-salt B88 and allowed to chill for 10 min with occasional swirling. Membranes were again sedimented, washed once with B88, and resuspended to 5.3 ml with B88. The membrane suspension was mixed with 5 ml of membrane-free cytosol (9 mg/ml), 1.32 ml of 10× ATP regeneration mix, and 1.6 ml of B88 to a final volume of 13.2 ml. The concentration of components was the same as described for stage II Transport. This mix is referred to as total, and was incubated 30 min at 25°C avoiding agitation of the sample. The reaction was chilled for 15 min, and a 12 ml MSS fraction was taken after sedimenting perforated cells at 12,000 *g* for 2 min at 4°C. All subsequent steps were carried out at 4°C. The MSS fraction was loaded in a 17 ml Ultraclear Beckman tube that contained 2 ml of 30% sucrose (wt/vol) layered on top of 2.5 ml of 60% sucrose, both dissolved in B88 without sorbitol. This tube, referred to as VS I, was subjected to overnight centrifugation (16 h) at 25,000 rpm in a Beckman SW41 rotor. The gradient was collected from the top at a rate of 0.3 ml/min using a gradient collector (Isco Inc.) and 9 × 1.5 ml fractions, followed by 30 × 0.2-ml fractions, were dispensed into siliconized microcentrifuge tubes (Sigma Chemical Co., St. Louis, MO). The absorbance at 280 nm was measured with a spectrophotometer (Isco, Inc.) attached to a 2 mm top-fitted flow cell. Aliquots (5 μl) of each fraction were mixed with 0.5 ml of water, and then with 5 ml of Universol ES scintillation fluid (ICN Biomedicals), and the radioactivity quantified in a Beckman scintillation counter. The peak of radioactivity, always centered around a density of 30% sucrose (wt/wt) was pooled (pool 1), avoiding fractions with a density above 32% sucrose (wt/wt). Pool 1 was adjusted to a density of 15% sucrose (wt/wt) by adding B88 without sorbitol. The diluted sample was loaded onto a 5 ml Ultraclear Beckman tube that contained a linear F gradient (prepared by layering 0.85-ml aliquots of 1% F/15% s, 2% F/15% s, 3% F/15% s, and 4% F/15% s, on top of 0.6 ml of 5% F/60% s, all dissolved in B88 without sorbitol, and

allowing it to stand at 4°C for 16 h). This tube, referred to as VS II, was subjected to centrifugation for 2 h at 40,000 rpm in a Beckman SW 50.1 rotor. The gradient was collected from the top as before, and 27 × 0.2-ml aliquots were collected into siliconized microcentrifuge tubes. The radioactivity in 5-μl aliquots of each sample was quantified as before. The peak of radioactivity was pooled (pool 2) adjusted to a density of 35% Nycodenz (wt/vol) by adding an equal volume of 80% Nycodenz, dissolved in B88 without sorbitol. The diluted sample was loaded in the bottom of a 5 ml Beckman Ultraclear tube, and layered with 0.7 ml aliquots of 30, 25, 20, 15, and 10% Nycodenz, all dissolved in B88 without sorbitol. This tube, referred to as EQ, was subjected to overnight centrifugation (16 h) at 40,000 rpm in a Beckman SW50.1 rotor. The gradient was collected as before, and 18 × 0.3-ml fractions were collected into siliconized microcentrifuge tubes. Aliquots (5 μl) were analyzed by scintillation counting, and the peak of radioactivity was pooled (pool 3).

Amido-black Protein Concentration Assay

Samples containing 0.1 to 10 μg of protein were diluted to 0.25 ml with distilled water, mixed with 0.03 ml of 1 M Tris, pH 7.5, 1% SDS, and then with 0.06 ml of 60% TCA (wt/vol). After 2 min at room temperature, the samples were spotted onto a nitrocellulose filter that was pre-soaked in 6% TCA and assembled into a Sigma dot blotter fitted to a vacuum hose. Sample wells were rinsed once with 6% TCA. Filters were removed from the dot blotter, rinsed with 6% TCA, and stained for 2–3 min in 0.1% amido black dissolved in MeOH/HOAc/H_2O (45:10:45). The stained filter was rinsed with distilled water, destained in MeOH/HOAc/H_2O (270:6:24), and soaked in distilled water. Protein spots were cut out and placed in siliconized microcentrifuge tubes that contained 0.3 ml of elution buffer (25 mM NaOH, 0.05 mM EDTA, 50% EtOH). After 20 min, the absorbance was read at 630 nm wavelength using a spectrophotometer (Perkin-Elmer, Corp., Norwalk, CT) fitted with 0.4 ml glass cuvettes. BSA was used as a standard protein to calculate sample concentrations.

^{125}I-Protein A Western Blots and Quantitation in PhosphorImager

Proteins in Laemmli sample buffer were heated at 65° or 95°C, resolved in 9 or 14% polyacrylamide gels, and transferred to nitrocellulose or Bio Rad PDVF membranes using a Bio Rad semi-dry blotter (75 min at 75 mA), or a minigel tank (Hoefer Scientific Instruments, San Francisco, CA) (2 h at 250 mA). Filters were stained with Ponceau S, rinsed in water, cut in sections, blocked with 2% milk in TBS-T for 30 min, and incubated with primary antibodies for 90 min. Blots were washed 4 × 7 min in TBS-T, and incubated with a 1:5,000 dilution of ^{125}I-protein A for 1 h at room temperature. Blots were washed 4 × 7 min, dried, and exposed to phosphor plates. The intensity of bands was quantified using standard software in a PhosphorImager (Molecular Dynamics).

GDPase Enzyme Assay

GDPase activity assays were performed as described in Yanagisawa et al. (1990). Samples (5–20 μl) were mixed with 100 μl of 20 mM imidazole-HCl, pH 7.4, 2 mM $CaCl_2$, 0.1% Triton X-100, and 10 mM GDP, or CDP as control. Tubes were incubated 30 min at 30°C and reactions were terminated by adding 150 μl of 2% SDS. Inorganic phosphate was quantified by the method of Friske-Subbarou. Samples were mixed with 750 μl of a 6:1 mix of 0.42% ammonium molybdate in 1 N H_2SO_4 and 10% ascorbic acid. The mix was incubated 20 min at 45°C, and the absorbance at 820 or 750 nm was determined using a Perkin Elmer or a Bio-Tek Instruments (Burlington, VT) spectrophotometers, respectively. GDPase activity is expressed as arbitrary units equivalent to absorption value.

TCA-DOC Protein Precipitation and Silver Stain Gels

Samples were diluted to 1 ml with distilled water in microcentrifuge tubes, mixed with 0.1 ml of 0.15% sodium deoxycholate, and then with 0.1 ml of 72% TCA. After 10 min at room temperature, precipitates were sedimented at 15,000 *g* for 15 min at 4°C, the tubes were decanted, and the pellets washed with chilled (−20°C) acetone. Precipitates were recollected by sedimentation as before, the tubes were decanted, and the pellets were allowed to dry at room temperature. Pellets were finally resuspended in 1× Laemmli sample buffer with 2% β-ME. Samples were heated to 65°C for 15 min, loaded in a 10 to 15% acrylamide-SDS gradient gel, and resolved by electrophoresis at 10–15 mA. Gels were fixed in 50% ethanol, 12% acetic acid, 0.02% formaldehyde for 1 h at room temperature. Fixed gels were washed 3 × 10 min with 50% ethanol, incubated for 1 min in 0.01% sodium thiosulfate, and then washed 3 × 15 s in distilled water. Gels were precoated for 20 min in 0.1% silver nitrate, then washed 2 × 20 s in distilled water, and finally developed for 3–6 min in 3% sodium carbonate, 0.02% formaldehyde, and 0.0002% sodium thiosulfate. Developed gels were rinsed 20 s in distilled water, and color development stopped by immersion and storage in 0.01 M EDTA, pH 8.0.

Immunoisolation of ER-derived Transport Vesicles

Aliquots (20–60 μl) of MSS fractions in 0.5 ml Eppendorf microcentrifuge tubes were incubated 1 h at room temperature with 1.25 μg of anti-Bet1 IgG or 0.5 μg of affinity purified anti-Sec22p antibodies (kind gift of Dieter Gallwitz, Max Planck Institute of Biophysical Chemistry, Göttingen, Germany). Protein A–Sepharose beads (5–10 μl of packed beads) were added, and tubes rotated for 1 h at room temperature. Beads were sedimented for 1 min at 2,000 rpm in a refrigerated microcentrifuge (Tomy Tech USA Inc.) and the supernatant fractions were saved. Beads were washed 4× with 0.4 ml of B88 and the samples were transferred to clean tubes during the first and last washes to minimize background. After decanting the last wash, proteins were extracted from beads with 1% Triton X-100 in B88 or 1× Laemmli sample buffer with or without reducing agent (2% β-ME). If Triton extracted, beads were washed twice more with 1% TX-100 in B88, and the remaining proteins were extracted with 1× Laemmli sample buffer with 2% β-ME at 70°C for 10 min.

Electron Microscopy

Negative Stain. Samples (6 μl) were spotted onto ionized copper grids that had a formvar support film stabilized by carbon, and were allowed to adsorb onto the film during a 15-min incubation at room temperature, in a humid chamber. Grids were washed gently in B88, and proteins were fixed during 15 min with 1% gluteraldehyde dissolved in B88. Grids were washed in distilled water and spotted with 10 μl of 2% uranyl acetate. Excess stain was removed and the grids were allowed to dry at room temperature. Stained particles were visualized and photographed using a Philips 301 electron microscope.

Thin Section. Aliquots (250 μl) of purified vesicles from pool 3 were diluted to 1 ml with B88, and sedimented at 100,000 *g* for 1 h onto a "bed" of hardened low-melting agarose (1 μl of 2.5%). After decanting, pellets were overlaid with 1% gluteraldehyde in B88 and allowed to fix for 1 h at 4°C. Pellets were washed 2 × 5 min with 0.1 M sodium phosphate, pH 7.4, and 2 × 5 min with 0.1 M veronal-sodium acetate, pH 7.6. Pellets were stained for 1 h at 4°C with 1% osmium tetroxide dissolved in veronal-sodium acetate pH 7.6, and then washed 3 × 5 min with 0.05 M sodium cacodylate, pH 7.0. Pellets were stained for 1 h at room temperature with 1% tannic acid dissolved in cacodylate buffer and then washed 3 × 5 min with 0.05 M veronal-sodium acetate, pH 6.0. Pellets were then stained 1 h at 37°C with 0.5% uranyl acetate in veronal acetate buffer, pH 6.0, and then washed 4 × 5 min with distilled water. Samples were dehydrated in a series of ethanol solutions of increasing concentration, and finally in 100% propylene oxide. Samples were embedded in low-viscosity Spurr resin, and allowed to polymerize overnight at 60°C. Silver/gold thin sections were cut and visualized using a Philips 301 electron microscope.

Preparation of Antibodies against Ypt1 and Bet1 Proteins

Ypt1p was overproduced in an *Escherichia coli* strain (Segev et al., 1988), isolated in inclusion bodies, solubilized with 8 M urea, and dialyzed against 0.1 M phosphate buffer, pH 7.4. A solution of Ypt1 protein (200 μg) was mixed 1:1 with Freund's complete adjuvant, and injected into rabbits. Rabbits were boosted monthly with 50 μg of antigen dissolved in Freund's incomplete adjuvant, and bled 2 wk after each injection. Anti-Ypt1p serum was used at a dilution of 1:2,000 in Western blots. A synthetic peptide that contains the NH_2-terminal 26 amino acids of Bet1p with an added cysteine at position 27 was used to prepare antibodies against Bet1p. Bet1 peptide was conjugated to BSA in a 10:1 molar ratio using the DSP cross-linker. Conjugates were gel filtered in a column that was equilibrated in 0.1 M phosphate buffer at pH 7.4. An aliquot of the conjugate (1 mg) was mixed 1:1 with Freund's complete adjuvant, and injected into rabbits. Rabbits were boosted monthly, twice with 500 μg of the conjugate in Freund's incomplete adjuvant, and twice more with 200 μg of unconjugated peptide. Rabbits were bled 2 wk after each boost. Anti-Bet1p serum was used at a dilution of 1:500 in western blots. IgG was purified using a protein A affinity matrix as described before (Harlow and Lane, 1988).

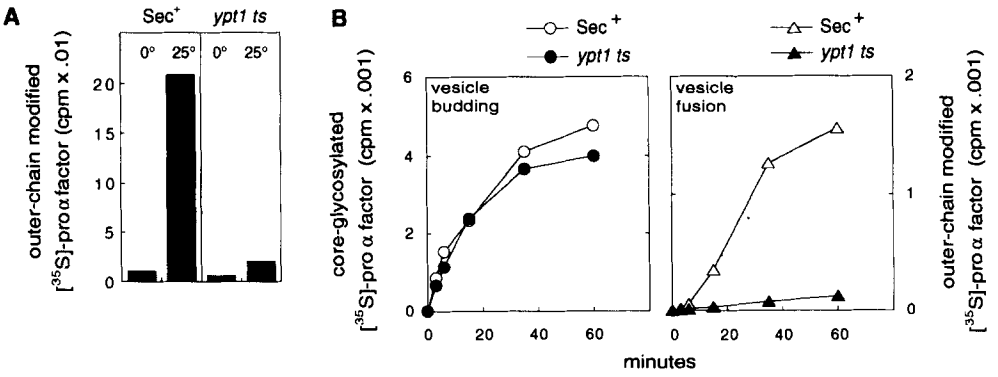

Figure 1. ER-derived transport vesicles accumulate in *ypt1* ts extracts. (*A*) Stage II reactions containing wild-type (*Sec*$^+$) or *ypt1* ts perforated cells and cytosol were incubated for 60 min at 0° or 25°C, as indicated. Chilled reactions were treated with trypsin and then trypsin inhibitor. Samples were heated in 1% SDS and the glycosylated pro-α-factor (*gpαf*) was quantified using precipitation with Con A and anti-outer-chain antibodies as described in the Methods for stage II transport. (*B*) Stage II reactions containing wild-type (*Sec*$^+$) or *ypt1* ts perforated cells and cytosol were incubated at 25°C for the indicated times, or at 0°C for the zero-time point control. Chilled samples were fractionated in a microcentrifuge into medium speed pellet and MSS fractions. MSS fractions were treated with trypsin and trypsin inhibitor, and processed for their content of gpαf as in *A*. The release of ^{35}S-gpαf from perforated cells (vesicle budding) is plotted in the left panel and the appearance of outer chain gpαf in the MSS (*vesicle fusion*) is plotted in the right panel. The zero time point of each set of MSS samples (less than 10% of the maximum signal) was subtracted as background from the corresponding MSS fractions to obtain the values shown.

Results

Review of In Vitro Reaction

Protein transport from the ER was reconstituted in perforated yeast spheroplasts using ^{35}S-radiolabeled ppαf as a marker secretory protein (Baker et. al., 1988). ppαf is post-translationally translocated into the lumen of the ER during a 15-min incubation at 10°C (stage I). Once in the ER lumen, pro-α-factor (pαf) is glycosylated with three N-linked core-carbohydrate chains which are then processed by a mannosidase and two glucosidases in the ER (Esmon et al., 1981; Abeijon and Hirschberg, 1992; Latterich and Schekman, 1994). After the membranes are washed to remove untranslocated precursor, the perforated cells are incubated at 20–29°C with a cytosol fraction, an ATP regenerating system, and GDP-mannose (stage II). During this stage, core-glycosylated pro-α-factor (core-gpαf) is transported to the Golgi apparatus where it is further glycosylated with "outer-chain" mannose residues in α1->6 linkage. All glycosylated forms of gpαf bind to the plant lectin Con A whereas all outer chain–modified forms of gpαf bind to antibodies specific to α1->6 linkages (Franzusoff and Schekman, 1989). Transport efficiency is expressed as the ratio of radiolabeled gpαf precipitated with outer chain antibodies to total gpαf precipitated with Con A.

Accumulation of Functional ER-derived Transport Vesicles

We previously showed that anti-Yptlp F_{ab} antibody fragments block ER to Golgi protein transport in perforated yeast spheroplasts and prevent the attachment of ER-derived transport vesicles to Golgi membranes. The Yptlp-specific block caused the accumulation of functional transport vesicles that were physically separable from ER and Golgi membranes (Rexach and Schekman, 1991). To obtain sufficient amounts of vesicles for purification, we needed to conduct large scale in vitro incubations. Large amounts of antibody F_{ab} fragments were required for repeated vesicle preparations. Therefore a mutation in the Ypt1 protein was used as an alternate inhibitor of Yptlp function. A strain that carries a mutant form of the Ypt1 protein (Schmitt et al., 1988) was examined for the ability to accumulate transport vesicles during in vitro incubations. The *ypt1* ts strain that we used for all experiments (referred to as *ypt1* ts throughout the text) carries an independent mutation in the glucosidase 1 gene (*gls1-1*) which renders the ER unable to trim terminal glucose residues from N-linked core-carbohydrate chains (Esmon et al., 1984). A mutation in the *GLS1* gene has no effect on cell growth, protein secretion, or outer chain modification (Esmon et al., 1984; Tsai et al., 1984), and was necessary to test whether diffusible ER-derived transport vesicles are competent for fusion with ER, as well as with Golgi membranes (see below).

Perforated cell and cytosol extracts were prepared from *ypt1* ts and wild-type strains, and tested for the ability to support ER to Golgi protein transport in the presence of ATP at physiologic temperature. *ypt1* ts extracts were 10 times less efficient than wild-type in reconstituted transport at 25°C (Fig. 1 *A*). To determine the stage of transport that is blocked in *ypt1* ts reactions, we examined the efficiency of vesicle budding and vesicle fusion. Vesicle budding was measured by quantifying the release of membrane-enclosed core-gpαf from perforated cells, and vesicle fusion was measured by quantifying the subsequent appearance of Golgi-modified forms of gpαf (Rexach and Schekman, 1991). Wild-type and *ypt1* ts cells had equivalent vesicle budding efficiencies (Fig. 1 *B*, *left*), but vesicle fusion was 10 times less efficient in the *ypt1* ts (Fig. 1 *B*, *right*). Thus, *ypt1* ts perforated cells produce transport vesicles, but fail to consume them.

Quantitative western blot analysis was used to measure the accessibility of ER-resident proteins to transport vesicles. After 35 min of vesicle budding, more than 35% of core-gpαf was incorporated into vesicles, compared to less than 5% of Kar2p (Fig. 2, *left*). Kar2p is a lumenal ER-resident protein, whereas core-gpαf is a soluble secretory proprotein (Rose et al., 1989; Julius et al., 1984). Likewise, 25% of Bet1p and 15% of Sec22p were incorporated into vesicles, compared to less than 2% of Sec61p (Fig. 2, *right*). Sec22 and Bet1 proteins are embedded in the ER membrane (Newman et al., 1992; Ossig, R., unpublished results) and

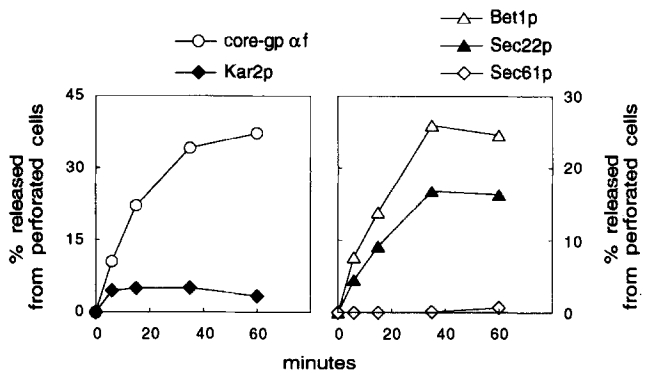

Figure 2. ER-resident proteins are sorted prior to the release of transport vesicles. Stage II reactions containing *yptl* ts perforated cells and cytosol were incubated at 25°C for the indicated times, or at 0°C for the zero time point control. Chilled samples were fractionated in a microcentrifuge, and MSS fractions were taken from the meniscus. One set of MSS fractions (*left*) was treated with trypsin and trypsin inhibitor, and heated at 95°C in 1× Laemmli sample buffer. Half of the sample was analyzed for its content of gpαf using precipitation with Con A as described in the Methods for stage II transport, and the other half was heated in 1× Laemmli sample buffer with 2% β-ME, subjected to SDS-PAGE, immunoblotted with anti-Kar2p antibodies (1:5,000) followed by ^{125}I-protein A, and the radioactivity was quantified using standard software in a Molecular Dynamics PhosphorImager. A second set of MSS fractions (*right*) was heated at 65°C in 1× Laemmli buffer with 2% β-ME, subjected to SDS-PAGE, and immunoblotted with anti-Sec61p (1:5,000), anti-Sec22p (1:5,000), and anti-Betlp (1:500) antibodies followed by ^{125}I-protein A, and quantitation in a PhosphorImager. The zero time point of each set of MSS samples was subtracted as background from the corresponding MSS fractions to obtain the values shown. Values shown in the right panel are the average of two separate experiments. An aliquot of an unfractionated reaction, referred to as "total," served to calculate the percent of each protein released from perforated cells.

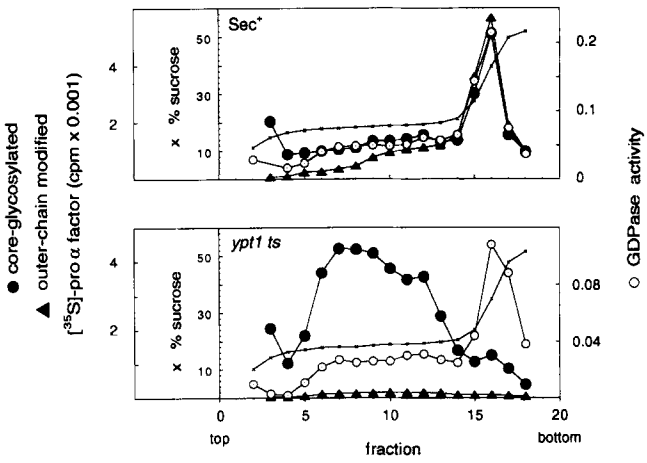

Figure 3. Transport vesicles that accumulate in *yptl* ts reactions are separable from Golgi membranes in F/s gradients. A scaled-up MSS fraction (300 μl) obtained from a wild-type (*Sec*$^+$) or *yptl* ts Stage II reaction was loaded in a F/s gradient (prepared as described in Materials and Methods) and subjected to centrifugation for 2 h at 100,000 *g*. 18 fractions were collected from the top. The gpαf content, GDPase activity, and the density of every fraction was quantified as described in Materials and Methods. Closed circles represent core-gpαf. Closed triangles represent outer-chain modified gpαf. Open circles represent GDPase activity. Crosses represent the density of each fraction expressed in % sucrose (wt/wt).

are components of ER-derived transport vesicles (see below), whereas Sec61 is a resident ER membrane protein (Stirling et al., 1992; Stirling, C., unpublished results). Based on these results, we concluded that sorting of proteins in the ER must occur prior to the scission of diffusible ER-derived transport vesicles.

We examined whether ER-derived vesicles that diffuse out of perforated cells during in vitro incubations were attached or not to Golgi membranes because Golgi membranes are also released from perforated cells during in vitro incubations. Vesicle targeting is measured by quantifying the percentage of core-gpαf in the MSS fraction that sediments slowly (within vesicles) or rapidly (with Golgi membranes) in velocity sedimentation gradients (Rexach and Schekman, 1991). Vesicles are marked by their content of ^{35}S-core-gpαf, whereas Golgi membranes are marked by their content of GDPase activity (Yanagisawa et al., 1990), and content of outer-chain-modified gpαf (Rexach and Schekman, 1991). Membranes released from wild type and *yptl* ts perforated cells after 35 min at 25°C were subjected to velocity sedimentation in Ficoll gradients (Fig. 3). In wild type reactions, all of the gpαf accumulated within membranes that sedimented fast, together with the majority of Golgi membranes (Fig. 3, *top*); half of the gpαf was outer-chain modified, and the other half remained core-glycosylated, possibly due to inefficient vesicle fusion or outer-chain glycosylation. Slowly-sedimenting membranes that contain GDPase activity may represent Golgi-derived transport vesicles. In *yptl* ts reactions, all of the gpαf remained core-glycosylated and accumulated within membranes that sedimented slowly, whereas the majority of Golgi membranes sedimented rapidly (Fig. 3, *bottom*). Thus, ER-derived vesicles are physically separable from large Golgi membranes that contain GDPase activity and accumulate outer chain gpαf. Small GDPase-containing vesicles were separated from ER-derived transport vesicles by velocity flotation in sucrose gradients (see Fig. 9 below).

Purification of ER-derived Transport Vesicles

Transport vesicles that accumulate in *yptl* ts extracts were purified using differential centrifugation and a combination of velocity and equilibrium density gradients. A flow diagram of the purification is shown in Fig. 4. A large mix of *yptl* ts perforated cells, cytosol, and an ATP regeneration system was incubated for 30 min at 25°C to generate ER-derived transport vesicles that contained ^{35}S-core-gpαf (see Materials and Methods). The chilled reaction mix was subjected to centrifugation at medium speed to remove perforated cells and the majority of cellular membranes. The MSS contained slowly sedimenting vesicles, and fragments of cellular membranes (see Table II below). Vesicles were concentrated by sedimentation onto a step sucrose gradient (referred to as VS I) and equilibrated as a single sharp peak at a density equivalent to 30% sucrose (wt/wt)(1.13g/ml) (Fig. 5, *top*). The peak of vesicles (28–32% sucrose) was pooled

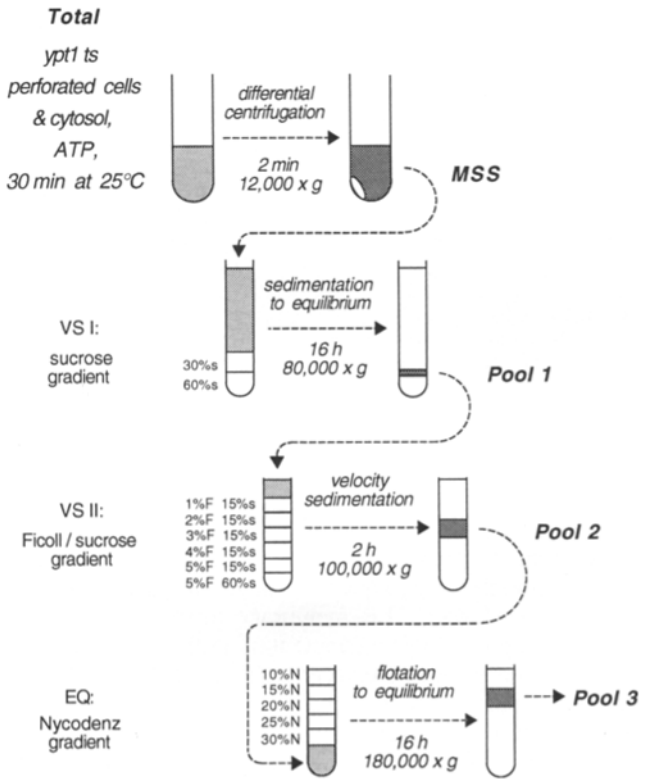

Figure 4. Flow diagram for the purification of ER-derived transport vesicles.

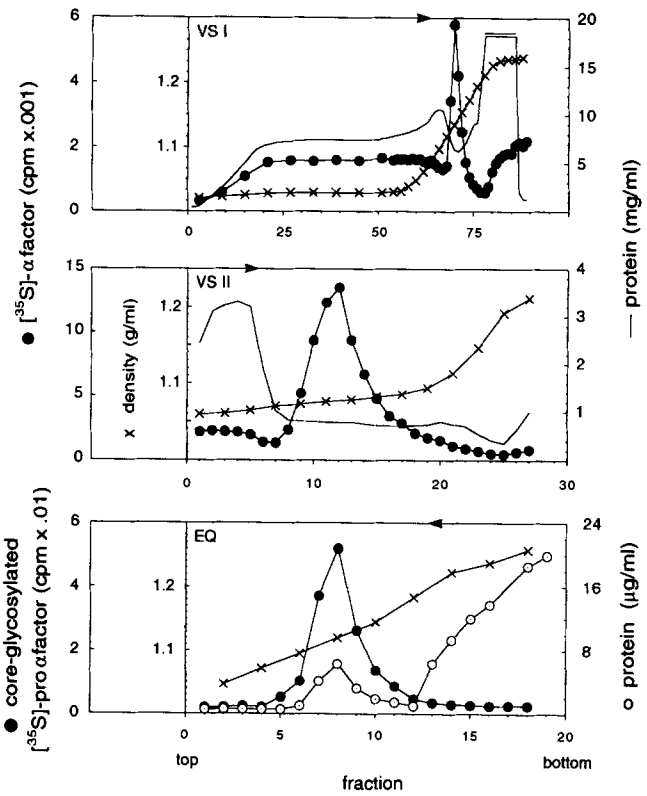

Figure 5. Purification of ER-derived transport vesicles. A large mix of *yptl* ts-perforated cells, membrane-free cytosol, and an ATP regeneration system was incubated for 30 min at 25°C, and then chilled (see Materials and Methods, and Fig. 4 for a flow diagram). Perforated cells were sedimented at 12,000 *g* for 2 min and the resulting MSS was loaded on top of a sucrose step gradient (VS I). Membranes were sedimented for 16 h at 80,000 *g*, and equilibrated at isopycnic densities. The peak of fractions that contained transport vesicles were detected by their content of radioactive core-gpαf and were pooled (pool *1*). The sample density was adjusted to 15% sucrose (wt/wt), loaded in a F/s gradient (VS II), and centrifuged at 100,000 *g* for 2 h. The vesicle peak was pooled as before (pool *2*). The sample density was adjusted to 35% Nycodenz, loaded in the bottom of a Nycodenz step gradient (*EQ*), and membranes floated to equilibrium during overnight centrifugation at 180,000 *g*. The vesicle peak was pooled as before (pool *3*), and analyzed. Closed circles represent radiolabeled forms of α factor in the top and middle panels, and core-gpαf in the bottom panel. Crosses represent solution density in grams per milliliter (*g/ml*). Smooth lines and open circles represent protein concentration. The arrows in the top x-axis point to the direction of membrane movement during sedimentation, and the arrow base marks the interface between load and gradient material.

(pool 1), the concentration of sucrose adjusted to 15% (wt/wt) by dilution, and the sample subjected to velocity sedimentation in a F/s gradient (referred to as VS II) that resolves membranes on the basis of size. Vesicles sedimented slowly as a single peak without reaching equilibrium density (Fig. 5, *middle*). The peak of vesicles was pooled (pool 2), the sample density was adjusted to 35% Nycodenz (wt/vol), and vesicles were floated to equilibrium in a Nycodenz density gradient (referred to as EQ) to remove all remaining soluble proteins and particles. The vesicles equilibrated as a single peak at a density of 1.12 g/ml (Fig. 5, *bottom*), and were pooled (pool 3).

To assess the purity of ER-derived transport vesicles, we measured the fold enrichment of transport vesicles and the recovery of cellular markers at each purification step. A purification chart is presented in Table I. Fold enrichment was determined by calculating the ratio of protease-protected core-gpαf to total micrograms of protein in each fraction. The value obtained for the total fraction was adjusted to reflect core-gpαf within vesicles, because a significant portion (Fig. 60%) of the core-gpαf in this fraction resided within ER membranes. We calculated that ER-derived transport vesicles were enriched 900-fold from the initial mix of perforated cells and cytosol. Quantitative ^{125}I-protein A Western blot analysis was used to determine the percent recovery of protein markers of cellular membranes and cytosol (Table II). The MSS contained slowly sedimenting vesicles, Golgi membranes, and detectable amounts of plasma membrane, vacuole, and mitochondrial markers. These contaminants were largely separated from ER-derived vesicles after isopycnic centrifugation in a sucrose gradient (Table II, *VS I*). Although detectable amounts of Golgi and vacuole membranes persisted throughout the purification, more than 99.5% of these membranes were removed (Table II, *Pool 3*).

ER-derived Transport Vesicles Fuse with cis-Golgi, but not with ER Membranes

The fusion competence of transport vesicles that accumulate in vitro was examined using assays that detected vesicle fusion to *cis*-Golgi, or to ER membranes. Because we used a glucosidase I–deficient *yptl*ts strain, the transport vesicles that accumulate in vitro contain the 32-kD "glucose-

Table I. Purification Table

Fraction	Volume	Protein	Core-glycosylated ^{35}S-pro-α-factor	Specific units	Enrichment	Recovery
	ml	*μg*	*cpm × 10⁻⁵*	*cpm × 10⁻²/μg*	*(-fold)*	*%*
Total	13	54,000	220/70	4.1/1.3		100
MSS	12	39,000	66	1.7	1.3	96
Pool 1	0.9	670	31	46	35	46
Pool 2	1.2	73	13	180	140	25
Pool 3	0.8	3.4	4.2	1,200	950	11

The content of protein and protease-protected gpαf (pp-gpαf) was determined for each purification step. The protein concentration in aliquots from each pool was determined using an amido-black protein detection assay (see Materials and Methods), and the content of protease protected ^{35}S-gpαf was determined by treating aliquots with trypsin, then trypsin inhibitor, followed by precipitation with Con A-Sepharose and quantitation in a scintillation counter, as for stage II transport reactions (see Materials and Methods). Two values are given for "core-glycosylated ^{35}S-pro-α-factor" and "specific units" in the total fraction: one indicates the total core-gpαf in the fraction (left value), and the other was adjusted to reflect the core-gpαf within diffusible vesicles (right value) and was deduced from the efficiency of vesicle budding (see "Vesicle budding and fusion assay" in Materials and Methods). Fold enrichment was calculated with respect to protease-protected core-gpαf within diffusible vesicles in the Total fraction. The values given for "percent recovery" were adjusted to account for sample aliquots taken throughout the purification. All values were rounded off to two significant figures after calculations were performed.

untrimmed" form of core-glycosylated pro-α-factor (referred to as *gls*-core-gpαf and core-gpαf throughout the text) instead of the 29-kD wild-type form. Altogether, nine glucose residues are trimmed from three N-linked carbohydrate chains to convert *gls*-core-gpαf to the wild-type form; a terminal glucose residue is removed by glucosidase I, and two more are removed by glucosidase II after the terminal glucose has been removed (Roth et al., 1990). The *glsl*-1 and wild type forms of core-gpαf are shown in Fig. 6 *A*, for reference. Fusion of ER-derived transport vesicles with wild-type ER membranes was measured by quantifying the percent glucose-trimming of radiolabeled *gls*-core-gpαf by glucosidase I and II in the ER lumen (see Latterich and Schekman, 1994), whereas fusion of vesicles with *cis*-Golgi membranes was measured by quantifying the conversion of radiolabeled *gls*-core-gpαf to "outer-chain" modified forms by α1,6 mannosyl-transferases in the *cis*-Golgi lumen (see review of in vitro assay; Rexach and Schekman, 1991). A sample homotypic ER–membrane fusion experiment is presented in Fig. 6 *B*, for comparison. Washed *glsl*-1 ER membranes that contained radiolabeled *gls*-core-gpαf were incubated with fresh wild-type ER membranes in the presence of various additions, and completed fusion reactions (except for reactions that contained Triton X-100) were treated with trypsin and then trypsin inhibitor to quantify membrane-enclosed gpαf (Fig. 6 *B*, lanes *1–3*). ER–membrane fusion reached 21% efficiency at physiological temperature in the presence (Fig. 6 *B*, lane *2*) but not in the absence (Fig. 6 *B*, lane *1*) of an ATP regeneration system, as judged by percent glucose trimming. Addition of cytosol neither stimulated nor inhibited ER–membrane fusion (not shown). When membrane barriers were removed by the presence of 1% Triton X-100 in the reaction, 92% of the *gls*-core-gpαf was trimmed (Fig. 6 *B*, lane *3*). A smear rather than a sharp band at 29 kD results from the addition of TX-100, which interferes with glucosidase activity. The smear may represent the nine intermediates in the conversion of core-gpαf from the *gls* to the wild-type form, and did not result from proteolysis of *gls*-core-gpαf, because a single species of deglycosylated proαfactor was formed when samples were treated with endo H (not shown).

ER-derived transport vesicles did not fuse with ER membranes. Glucose trimming was not detected when aliquots of isolated vesicles (from pool 1) were incubated at physiological temperature with an ATP-regeneration system and wild-type microsomes that contained fusion-competent ER membranes (Fig. 6 *C*, lanes *2* and *2'*). These conditions normally

Table II. Recovery of Cellular Markers

Marker protein	Cellular location	Total	MSS	Pool 1 (Percent recovery)	Pool 2	Pool 3
core-gpαf	lum ERV	100	96	46	25	11
Sec61p	tm ER	100	7	0	0	0
GDPase	tm Golgi	100	37	3.4	1.2	0.4
VPM1	tm Vac	100	29	2.9	0.7	0.1
PM ATPase	tm PM	100	17	0	0	0
F1Bo	pm Mito	100	28	0	0	0
PGK	sol Cyt	100	88	0.3	0	0

Aliquots of Total and MSS fractions that contained 31.25, 6.25, and 1.25 micrograms of protein, and aliquots of pools 1, 2, and 3 fractions that contained 1.25, 0.25, and 0.05 μg of protein, respectively, were subjected to SDS-PAGE, and immunoblotted with anti-Sec61p (1:5,000), anti-PGK (1:10,000), anti-PM ATPase (1:1,000), anti-VPM1 (1:500), and anti-F1Bo (1:1,000) antibodies. Immune-complexes were detected by ^{125}I-protein A and quantified in a PhosphorImager; the values obtained were expressed as disintegrations per μl of sample analyzed, and were used to calculate the % recovery of each marker after each purification step. In the case of core-gpαf, values were calculated as in Table I. Values obtained in GDPase assays (see Materials and Methods), were expressed as units of enzyme activity per μl of sample analyzed, and were used to calculate % recovery. Core-gpαf is a lumenal (*lum*) marker of ER-derived transport vesicles (*ERV*); Sec61p is a transmembrane (*TM*) protein that marks the endoplasmic reticulum (*ER*); guanosine diphosphatase (*GDPase*) marks the Golgi complex (Golgi); an integral membrane component of the vacuolar proton pump (*VPM1*) marks the yeast vacuole (*Vac*); plasma membrane ATPase (*PM ATPase*) marks the plasma membrane (*PM*); a subunit of the mitochondrial proton pump (*F1Bo*) is a peripheral membrane (*pm*) protein that associates tightly with the mitochondrial membrane (*Mit*); phosphoglycerolkinase (*PGK*) is a soluble (*sol*) protein in the cytosol (*Cyt*).

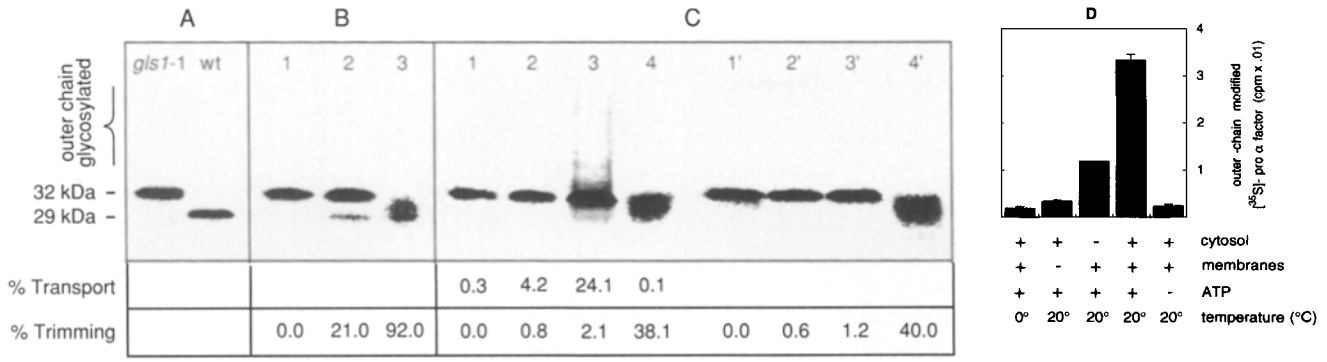

Figure 6. Fusion competence of ER-derived transport vesicles. (*A*) Phosphor-image displaying *gls*-core-gpαf and wild-type core-gpαf. Radiolabeled ppαf was translocated at low temperature into microsomes prepared from *glsl*-1 or wild-type yeast, as indicated. Chilled microsomes were washed, treated with trypsin and trypsin inhibitor, mixed with 2× Laemmli sample buffer with 2% β–ME, heated to 95°C, and resolved in a 12.5% SDS-PAGE. The gel was fixed, dried, exposed to a phosphor plate, and visualized in a Molecular Dynamics PhosphorImager. (*B*) Control reactions to test the fusion-competence of ER membranes. Washed *glsl*-1 microsomes (75 μg) that contained radiolabeled *gls*-core-gpαf (prepared as in A) were mixed with microsomes (75 μg) prepared from wild-type (lane *1–3*), and with an ATP regeneration system (lane 2) or 1% Triton X-100 (lane *3*) in a total volume of 50 μl. Reactions were incubated for 60 min at 30°C. Chilled reactions were treated with trypsin, and then trypsin inhibitor, and processed as in *A*. The percent trimming (conversion of the 32-kD *gls*-core-gpαf to the 29-kD wild-type form) was quantified using standard software in a Molecular Dynamics PhosphorImager. (*C*) Fusion competence of isolated transport vesicles. Aliquots (5 μl) of an enriched transport vesicle preparation (from pool *1*) were mixed with 25 μg of wild-type yeast microsomes, an ATP regeneration system, and 100 μg of cytosol (unless otherwise indicated) in the presence (lanes *1–4*) or absence (lanes *1′–4′*) of GDP-mannose. The reactions in lanes *2* and *2′* did not contain cytosol. Reactions were incubated for 1 h at 0°C (lanes *1* and *1′*) or 20°C (lanes *2–3* and *2′-3′*). Chilled reactions were treated with trypsin and trypsin inhibitor, and processed as in *A*. The percent trimming was quantified as before, and the percent transport was quantified using precipitation with Con A and anti-outer-chain antibodies as described in the Methods for stage II transport. (*D*) Fusion competence of purified transport vesicles. Aliquots of purified transport vesicles (from pool *3*) were mixed or not with fresh cytosol and perforated spheroplasts prepared from wild-type cells, and an ATP regeneration mix, to the same concentrations as for stage II transport. To the tubes containing no ATP, we added apyrase (0.5 U) to hydrolyze residual ATP; these tubes were supplemented with 50 μM GDP-mannose, normally added in the ATP regeneration mix. Samples were incubated for 1 h at 0° or 20°C, and reactions terminated by the addition of 2% SDS and heated to 95°C. Samples were processed for precipitation with Con A and anti-outer chain antibodies as described in the Materials and Methods for stage II transport.

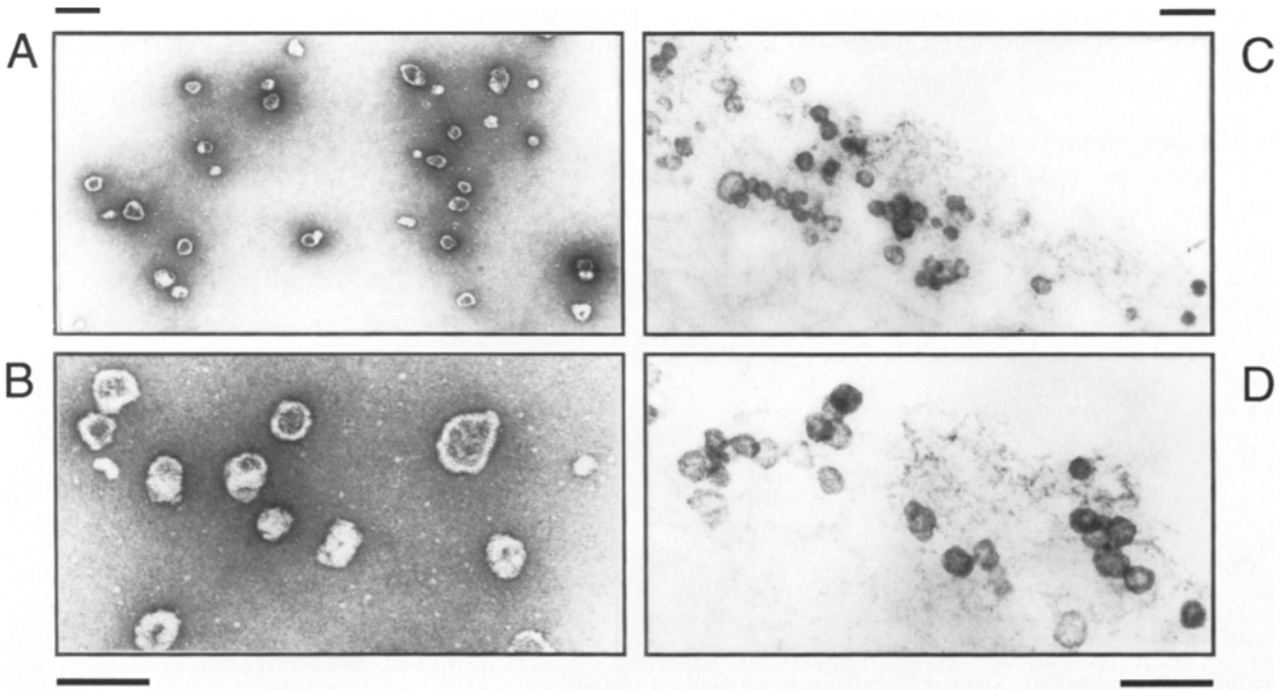

Figure 7. Morphology of ER-derived transport vesicle examined under the electron microscope. *A* and *B* show purified vesicles from pool 3 that were attached to an ionized support grid, fixed, and visualized by negative stain with 2% uranyl acetate. *C* and *D* show vesicles from the same pool 3 that were sedimented onto a hardened agarose "bed" and processed for thin section electron microscopy. Magnifications were 25,000× in *A*, 57,000× *B*, 34,000× *C*, and 57,000× *D*. Bars, 200 nm.

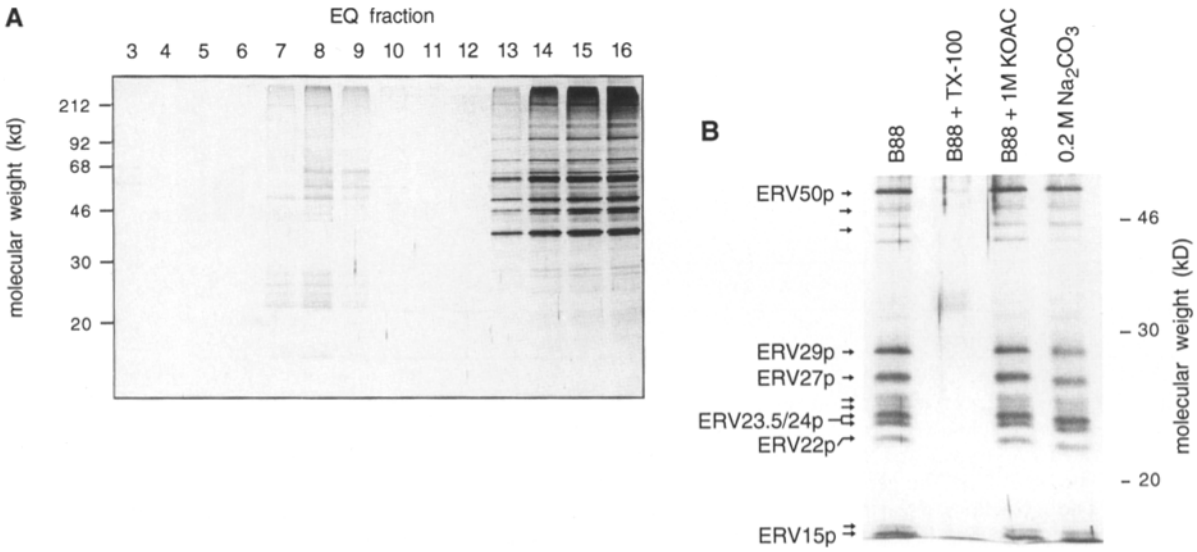

Figure 8. Polypeptide composition of ER-derived transport vesicles. (*A*) Protein from each fraction of the Nycodenz equilibrium gradient (*EQ*) was concentrated by precipitation with trichloroacetic acid in the presence of deoxycholate, resolved in a 10–15% acrylamide gradient gel, and stained with silver (see Materials and Methods). (*B*) Aliquots of pool 3 were diluted 10-fold in tubes with the indicated solutions (B88 is 20 mM Hepes, pH 6.8, 150 mM KOAc, 250 mM sorbitol, 5 mM MgOAc). A 1% Triton X-100 solution was used. Sodium carbonate was dissolved in water. After 10 min at room temperature, vesicles were sedimented at 100,000 *g* for 45 min. The pellets were resuspended in Laemmli sample buffer with 2% β-ME, and the proteins resolved by SDS-PAGE and visualized by silver stain. Arrows indicate the most abundant vesicle proteins, and some were assigned apparent molecular mass. ERVp is an abbreviation for ER-derived transport Vesicle protein.

support efficient ER-membrane fusion (Fig. 6 *B*, lane *2*). Addition of cytosol did not stimulate "back-fusion" (Fig. 6 *C*, lanes *3* and *3'*). Glucosidase activity was present in membranes because 40% of the *gls*-core-gpαf was trimmed when membrane barriers were removed by the presence of 1% Triton X-100 (Fig. 6 *C*, lanes *4* and *4'*).

Transport vesicles were active for fusion with *cis*-Golgi membranes. Completion of protein transport was detected when aliquots of isolated vesicles (from pool 1) were mixed with cytosol, an ATP-regeneration system, GDP-mannose, and wild-type microsomes that contained fusion-competent *cis*-Golgi membranes (Fig. 6 *C*). Vesicle fusion with *cis*-Golgi membranes was not detected at 0°C (Fig. 6 *C*, lane *1*), but reached 24% efficiency at 20°C (Fig. 6 *C*, lane *3*) in a

Table III. Fold Enrichment of Transport Proteins

Protein	Cellular location	Total	MSS	Pool 1 (fold enrichment)	Pool 2	Pool 3
core gpαf	lum ER/ERV	1	0.49/1.3	24/62	48/130	320/840
Sec13p	pm cyt	1	0.88	0.62	0	0
Sec17p	pm cyt	1	0.87	0.99	2.7	0
Sec21	pm cyt	1	1.4	2.7	2.5	0
Sec22p	tm ER/ERV	1	0.23/1.3	3.7/21	9.4/53	81/450
Sec23p	pm cyt	1	4.5	2.8	0	0
Arf1,2p	pm cyt/Golgi	1	1.2	0	0	0
Sar1p	pm cyt/ER	1	0.26	0	0	0
Ypt1p ts	pm cyt/Golgi	1	0.95	0.68	0	0
Bet1p	tm ER/ERV	1	0.62/1.3	4.7/10	13/28	210/450
Sly1p	pm cyt	1	0.67	5.4	0	0
α-COP	pm cyt	1	1.6	12	13	10
β/β'/γ-COP	pm cyt	1	1.7	5.0	6.1	5.9
δ-COP	pm cyt	1	1.7	8.2	6.7	3.5

Aliquots of total and MSS fractions that contained 31.25, 6.25, and 1.25 μg of protein, and aliquots of pools 1, 2, and 3 fractions that contained 1.25, 0.25, and 0.05 μg of protein, respectively, were subjected to SDS-PAGE and immunoblotted with anti-Sec13p (1:1,000), anti-Sec17p (1:2,000), anti-Sec21p (1:1,000), anti-Sec22p (1:5,000), anti-Sec23p (1:1,000), anti-Arfp (1:1,000), anti-Sar1p (1:1,000), anti-Ypt1p (1:2,000), anti-Bet1p (1:500), anti-Sly1p (1:1,000), and anti-coatomer (1:5,000) antibodies. Immune-complexes were detected by ^{125}I-protein A and quantified in a PhosphorImager; the values obtained were expressed as disintegrations per μg of protein analyzed, and served to calculate the values shown. Fold enrichment was calculated with respect to the amount of each marker in the total fraction, which was normalized to a value of 1. The values presented for core-gpαf were obtained by PhosphorImager quantitation of triply glycosylated ^{35}S-core-gpαf in nitrocellulose filters; these values include core-gpαf that is not protease protected. Two values for fold enrichment are given for proteins that are highly enriched in transport vesicles: the value on the left indicates the fold enrichment with respect to the amount of marker in the total fraction, and the value on the right indicates fold enrichment calculated with respect to the amount of marker within diffusible vesicles in the total fraction.

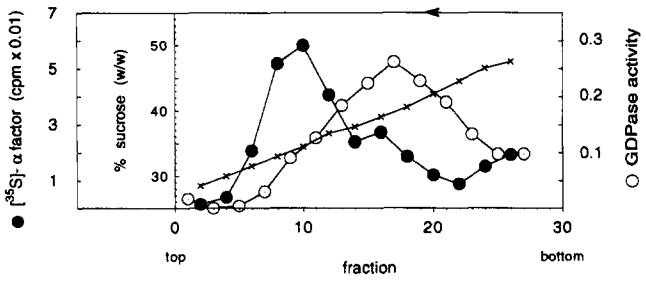

Figure 9. ER-derived transport vesicles are physically separable from Golgi-derived vesicles. Membranes that sediment slowly in velocity sedimentation gradients (Fig. 3, *bottom*, lanes *6–12*) were pooled and the solution density was adjusted to 50% sucrose (wt/vol). The sample was loaded in the bottom of a 5 ml Beckman Ultraclear tube, and aliquots of 45, 40, 35, and 30% sucrose were layered on top, all dissolved in B88. Membranes floated towards equilibrium during 20 h of centrifugation at 180,000 *g*. Isopycnic equilibration required more than 32 h of centrifugation (not shown). Aliquots were analyzed for their content of radiolabeled α-factor, GDPase activity, and density as described in the Materials and Methods.

reaction that required cytosolic protein (Fig. 6 *C*, compare lanes *2* and *3*) and the presence of intact membranes (Fig. 6 *C*, compare lanes *3* and *4*). The heterogeneous smear above the 32-kD *gls*-core-gpαf band represented outer chain–modified gpαf, and its formation required the presence of GDP-mannose in the reaction (Fig. 6 *C*, compare lanes *3* and *3'*). Purified transport vesicles remained active for fusion with *cis*-Golgi membranes. Completion of protein transport was detected when aliquots of purified vesicles (pool 3) were mixed with fresh perforated cells and cytosol prepared from a wild-type strain (Fig. 6 *D*). Transport required the addition of Golgi membranes and ATP, and was stimulated by cytosol. Transport was not detected at 0°C, but reached 22% efficiency at 20°C. The efficiency of transport from purified vesicles was comparable to the initial efficiency of transport from vesicles in the MSS fraction (not shown) and Pool 1 (Fig. 6 *C*, lane *3*).

Morphology of ER-derived Transport Vesicles

Fig. 7 shows typical electron micrographs of transport vesicles visualized by negative stain (*A* and *B*) and thin-section microscopy (*C* and *D*). Purified vesicles in pool 3 were attached to ionized support grids, fixed, and stained with uranyl acetate; pool 3 contained a uniform population of vesicles that collapsed during dehydration, indicative of the absence of a rigid structural coat (Fig. 7, *A* and *B*). Vesicles from the same pool 3 were sedimented onto a hardened agarose "bed," fixed, and processed for thin-section electron microscopy. An agarose "bed" was used because vesicle pellets were otherwise invisible. The vesicles were ~60 nm in diameter, lacked apparent protein coats surrounding the membrane, and were aggregated as a result of sedimentation (Fig. 7, *C* and *D*).

Molecular Composition of ER-derived Transport Vesicles

The protein composition of purified vesicle fractions was analyzed by SDS-PAGE, and visualized by silver stain. Proteins in aliquots of fractions from the last gradient (EQ) were concentrated by precipitation with trichloroacetic acid in the presence of deoxycholate, resolved in a 10 to 15% acrylamide-SDS gradient gel, and stained with silver (Fig. 8 *A*). The protein composition of fractions that contained transport vesicles was highly simplified (fractions *7–9*), and clearly distinct from the load (fractions *13–16*) and fractions from all previous purification steps (not shown; see MSS in Fig. 10, lane *1*). The 68/55-kD protein doublet in fractions 3, 8, 9, and 10 was human keratin introduced by sample handling. The most abundant vesicle proteins were assigned an apparent molecular mass and were named "ERV" proteins, an abbreviation for ER-derived transport vesicle proteins. ERV proteins were tightly associated with the vesicle membrane and resisted extraction with 1M KOAc or 0.2 M Na_2CO_3 at pH 11, but not with 1% TX-100 (Fig. 8 *B*).

The enrichment or depletion of various proteins that function in ER to Golgi protein transport in vivo was determined for each purification step using quantitative ^{125}I-protein A Western blot analysis (Table III). Sec13, Sec23, and Sar1 proteins were resolved early in the purification; these are peripheral membrane proteins that function to drive vesicle budding from ER membranes (Salama et al., 1993) and can form a coat around ER-derived transport vesicles (Barlowe et al., 1994). In contrast, Bet1 and Sec22 proteins were enriched 450-fold; these are membrane-embedded proteins with structural similarity to synaptobrevin (Dascher et al., 1991). Bos1p was enriched to the same extent as Sec22p, judged by ECL-Western blot analysis (not shown). Sec22 and Bos1 proteins function in transport vesicle docking or fusion with Golgi membranes (Kaiser and Schekman, 1990; Shim et al., 1991; Lian and Ferro-Novick, 1993). Subunits of yeast coatomer were also detected in purified vesicle fractions and were slightly enriched. We calculated that coatomer constituted only 1% of the vesicle protein by comparison to known amounts of purified coatomer (Hosobuchi et al., 1992) in ^{125}I-Western blots (not shown). Arf proteins were absent in purified vesicle fractions; these proteins function in the recruitment of coatomer and clathrin to membranes (Palmer et al., 1993; Stamnes and Rothman, 1993). Although Yptlp is suspected of binding ER-derived transport vesicles (Segev, 1991; Lian and Ferro-Novick, 1993), the mutant form of Yptlp used in this study was not detected in vesicles, perhaps due to its inability to bind GTP (Wagner et al., 1987). Finally, neither Sec17 nor Sly1 proteins were detected in purified vesicle fractions. Sec17p/αSNAP is a peripheral membrane protein that functions in transport vesicle docking or fusion (Kaiser and Schekman, 1990; Clary et al., 1990; Griff et al., 1992) and Slylp is a peripheral membrane protein that when mutated can replace Yptlp function (Dascher et al., 1991).

Because purified vesicle fractions contained detectable amounts of Betlp, Sec22p, Boslp, coatomer, and GDPase (see Tables II and III), we applied other techniques to determine whether these proteins were components of the same vesicles. Small Golgi vesicles that contained GDPase cofractionated with ER-derived transport vesicles in velocity sedimentation (Fig. 2) and equilibrium density gradients (not shown), but were separated by velocity flotation in sucrose gradients (Fig. 9). GDPase-containing vesicles floated towards equilibrium at a slower rate than ER-derived trans-

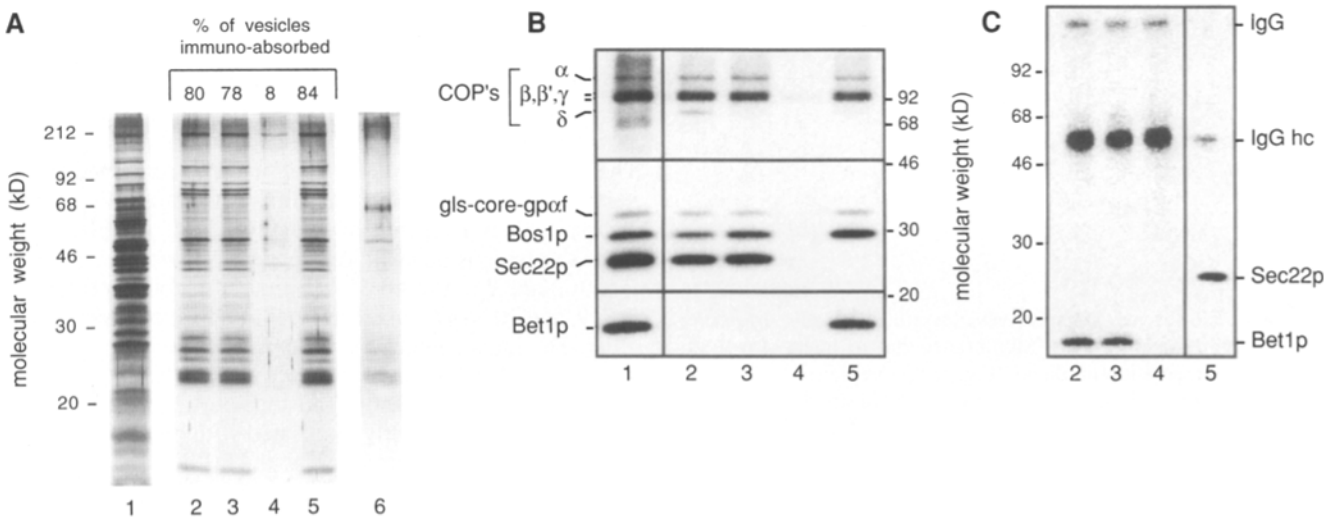

Figure 10. Core-gpαf, Betlp, Sec22p, Boslp, and coatomer reside in the same vesicles. Vesicles in MSS fractions from *yptl* ts stage II incubations were immunoadsorbed onto protein A-Sepharose beads using anti-Betlp IgG (lanes *2–4*, *A–C*) or anti-Sec22p affinity-purified antibodies (lane *5*, *A–C*). Immunoadsorbtions were conducted for 2 h in the absence of competitor peptides (lanes *2* and *5*, *A–C*) or in the presence of the RTQLFG competitor peptide (lane *3*, *A–C*) or the Betl immune-peptide (lane *4*, *A–C*). At the end of the incubations the beads were sedimented, the supernatants were saved, and beads were washed repeatedly in preparation for detergent extractions. (*A*) Top insert. Immunoisolates and supernatant fractions (unbound) were treated with trypsin and then trypsin inhibitor, and processed for Con A precipitation as described in stage II transport in the Materials and Methods. Immunoadsorbtion of ER-derived transport vesicles to Sepharose beads is expressed as the per cent of the ratio of protease protected core-gpαf (pp-core-gpαf) in immunoisolates divided by the summation of pp-core-gpαf in the supernatant and immunoisolate fractions. (A) Gel. Vesicle proteins were extracted from beads with 1% Triton X-100 in B88, resolved by SDS-PAGE, and visualized by silver stain (lanes *2–5*, panel *A*). A diluted aliquot of a MSS fraction was loaded in lane *1* of the same gel for comparison; it is underexposed in relation to lanes *2–5*. An aliquot of gradient-purified vesicles (from pool *3*) was loaded in lane *6* of the same gel, for comparison; it is overexposed in relation to lanes *2–5*. (B) Vesicle proteins were extracted from beads with 1% Triton X-100 in B88, resolved by SDS-PAGE, and visualized by Phosphorimaging of ^{125}I-protein A Western blots using anti-Betlp (1:500), anti-Sec22p (1:5,000), anti-Boslp (1:2,000), and anti-coatomer (1:5,000) antibodies. Gradient-purified vesicles from pool 3 (0.3 mg) were diluted fivefold in B88, sedimented to a pellet at 100,000 *g* for 45 min, resuspended in sample buffer, and loaded in lane *1*. *gls*-core gpαf is visible because it is labeled with [^{35}S]methionine. (C) After extracting vesicle proteins from beads with 1% Triton X-100 dissolved in B88, beads were washed twice more with the same buffer, and the remaining proteins extracted with 1× Laemmli sample buffer with 2% β-ME at 70°C for 15 min. SDS extracts were analyzed by SDS-PAGE, and visualized by Phosphorimaging of western blots using anti-Betl (lanes *2–4*) or anti-Sec22 antibodies (lane *5*) at the same dilution as in *B*. Heavy chain IgG is visible because it binds ^{125}I-protein A. Contiguous panels are from the same gel. Each panel was blotted separately with an antibody, or antibody mix in the case of Sec22 and Boslp, at the same dilution as in *B*.

port vesicles. Because the protein composition of GDPase-containing membranes could not be detected by silver stain (not shown), we believe that these membranes represent a small contaminant in purified vesicle preparations.

Antibodies that recognize Betlp or Sec22p were used to adsorb vesicles from MSS fractions onto protein A–coated Sepharose beads, and the presence of core gpαf, Betlp, Sec22p, Boslp, and coatomer on immunoisolates was examined by Western blot analysis (Fig. 10). Vesicles were marked by their content of protease-protected, radiolabeled *gls*-core-gpαf. An IgG fraction of antibodies prepared against the NH_2 terminus of Betlp (see Materials and Methods) efficiently adsorbed 80% of ER-derived transport vesicles to Sepharose beads (Fig. 10 *A* top insert, lane *2*). Betlp contains a six amino acid sequence (RTQLFG) in its NH_2 terminus that is also present in Boslp; consequently, the anti-Betlp antibodies have a low titer against Boslp. Although affinity purification against the immune-peptide would not select against cross-reacting antibodies, a 9–amino acid peptide that contains the common sequence RTQLFG efficiently competed antibody recognition of Boslp but not Betlp in immune-adsorption experiments (see below; Fig. 10 *B*, compare lanes *2* and *3*) and ECL-Western blots (not shown). Addition of the RTQLFG peptide did not affect the efficient (80%) immuno-isolation of vesicles by anti-Betl IgG (Fig. 10 *A*; top insert, compare lanes *2* and *3*), but the Betl immune-peptide fully prevented immune-adsorption (lane *4*). Pre-immune IgG precipitated nothing (not shown). The specificity of the anti-Betlp antibody was confirmed in an experiment described below and in the results shown in Fig. 10 *C* (lanes *2–4*). In addition, we used antibodies prepared against the cytoplasmic domain of Sec22p and affinity purified on nitrocellulose filters that contained *E. coli*-overproduced Sec22p fragments. Anti-Sec22p antibodies adsorbed 84% of ER-derived transport vesicles to Sepharose beads (Fig. 10 *A*; top insert, lane *5*). Although an immune-competition experiment was not possible because cytoplasmic fragments of Sec22p were insoluble, the specificity of the antibody was documented by the immunoblot shown in Fig. 10 *C* (lane *5*).

The protein composition of vesicles in immunoisolates was examined. Vesicle proteins were extracted from beads with 1% Triton X-100, resolved by SDS-PAGE, and visualized by silver stain (Fig. 10 *A*, gel). The protein composition

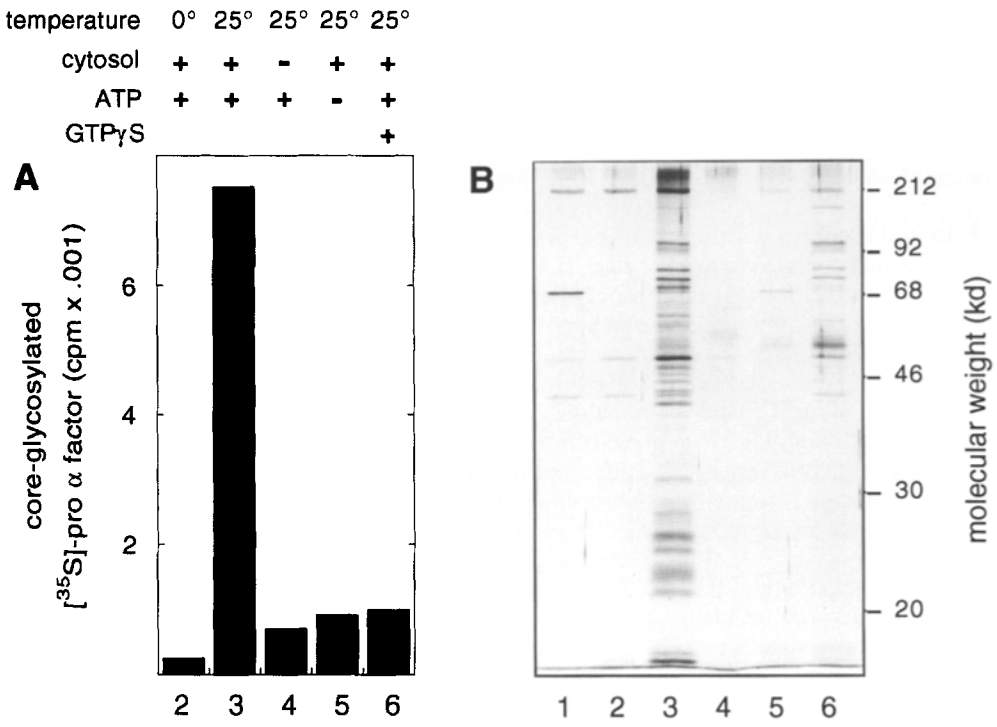

Figure 11. Transport vesicles form de novo during in vitro incubations. After stage I, *ypt1* ts membranes were washed and aliquoted into tubes that contained the indicated components, to the same concentration as for stage II (see Materials and Methods). Reaction volumes were adjusted to 50 μl with B88. To the tubes containing no ATP, we added apyrase (0.5 U) to hydrolyze residual ATP; these tubes were supplemented with 50 μM GDP-mannose, normally added in the ATP regeneration mix. GTPγS was added to a concentration of 80 μM. After 35 min of incubation at 25°C, perforated cells were sedimented in a microcentrifuge, and vesicles in MSS fractions were immunoisolated with anti-Betlp antibodies as described in Fig. 10. Cytosol (180 μg) was used instead of an MSS fraction for lane *1*. The protein composition of immunoisolates was visualized by silver stain as before.

of vesicles immunoisolated with anti-Betl or anti-Sec22 antibodies was indistinguishable (Fig. 10 *A*, lanes *2*, *3*, and *5*) and clearly distinct from the protein composition of MSS fractions (lane *1*). Immunoisolated vesicles contained all of the ERV proteins present in gradient-purified vesicles (Fig. 10 *A*, compare lane *6* with lanes *2*, *3*, and *5*), and several other abundant proteins. The Betl immune-peptide (Fig. 10 *A*, lane *4*), but not the RTQLFG peptide (lane *3*), prevented the adsorption of vesicle proteins to beads. The presence of Betlp, Sec22p, Boslp, and coatomer in immunoisolates was tested using western blot analysis (Fig. 10, *B* and *C*) and the relative amount of each protein was compared to that in 0.3 μg of gradient-purified vesicles (Fig. 10 *B*, lane *1*). Triton X-100 extracts of anti-Betlp immunoisolates (Fig. 10 *B*, lanes *2* and *3*) contained Sec22p, Boslp, core-gpαf, and coatomer. Addition of RTQLFG peptide to antibodies prior to immunoisolation prevented the partial (40%) adsorption of Boslp by cross-reacting antibodies (Fig. 10 *B*, compare lanes *2* and *3*), whereas addition of Betl immune-peptide prior to immunoisolation fully prevented adsorption of vesicles to beads (lane *4*). Antibody–antigen complexes were not extracted from beads by Triton X-100, but were subsequently extracted with 1% SDS at 65°C (Fig. 10 *C*). Betlp–IgG protein complexes were recovered from beads in SDS extracts (Fig. 10 *C*, lanes *2* and *3*), except when Betl-immune peptide was mixed with antibodies prior to immunoisolation (lane *4*). The Boslp that was adsorbed onto beads by cross-reacting antibodies was also recovered in the SDS extracts and could be detected with anti-Boslp antibodies (not shown). Triton X-100 extracts of anti-Sec22p immunoisolates contained Betlp, Boslp, core-gpαf, and coatomer (Fig. 10 *B*, lane *5*), and Sec22p-IgG complexes were recovered from beads in SDS extracts (Fig. 10 *C*, lane *5*).

Immunoisolation with anti-Betlp antibodies was used to examine the requirements for the formation and release of vesicles. The release of ER-derived transport vesicles from *ypt1* ts perforated cells required cytosol, an ATP regeneration system, physiologic temperature, and the absence of GTPγS (Fig. 11 *A*; Rexach and Schekman, 1991). Membranes that contain ERV proteins were released from perforated cells with the same biochemical requirements as ER-derived transport vesicles (Fig. 11 *B*) and were not present in the cytosol fraction used to promote vesicle budding (lane *1*).

Discussion

We provide a direct biochemical demonstration that diffusible vesicles mediate the selective and vectorial transport of secretory proteins from ER to Golgi membranes. This required the purification of functional ER-derived transport vesicles, assays that reconstitute ER-membrane fusion and vesicle fusion with *cis*-Golgi membranes, and a molecular comparison of transport vesicle and donor membranes to establish differences in composition. A specific inhibitor of vesicle targeting was necessary to accumulate ER-derived transport vesicles that were amenable to purification, because these are only transient intermediates in reconstituted

transport (Figs. 1 and 3). Inhibition of Yptl-function by specific antibodies (Rexach and Schekman, 1991) or by mutation (this study) was suitable, since it had no effect on the formation and release of transport vesicles from ER membranes (Fig. 1), but prevented vesicles from forming stable interactions with Golgi membranes (Fig. 3). ER-derived transport vesicles that formed in Yptlp-deficient reactions were physically separable from ER and Golgi membranes, and were free to diffuse out of perforated cells through holes in the plasma membrane. These conditions allowed the purification of vesicles which were monitored by their content of ^{35}S-core-gpαf.

Evidence demonstrates that ER-derived transport vesicles were purified extensively. First, vesicles that contained protease protected core-gpαf were enriched 950-fold from a mix of perforated cells and cytosol (Table I). Second, the peak of transport vesicles coincided precisely with the peak of protein in the last purification step (Fig. 8 *A*). Third, electron microscopy shows a uniform population of 60 nm vesicles with only occasional larger membrane impurities (Fig. 7). Finally, protein markers of cytosol, ER, and Golgi membranes, as well as vacuole, mitochondria, and plasma membranes, were virtually absent in purified vesicle preparations (Table II).

Several lines of evidence establish the authenticity of the purified ER-derived transport vesicles. Transport vesicles contained only ER-modified forms of α factor and accumulated only when reconstituted ER to Golgi protein transport was blocked by a specific inhibitor (Figs. 1 and 3). Purified transport vesicles were 60 nm in size, as are the putative transport vesicles that accumulate in vivo in a subset of yeast mutant strains that are blocked in ER to Golgi protein transport (Kaiser and Schekman, 1990). The vesicles purified were not fragments of ER or Golgi membranes because they lacked protein markers of these membranes. Vesicles did not contain Sec61p or Kar2p; these proteins are dispersed throughout the ER network, mark the ER membrane and lumen, respectively, and function in protein translocation into the ER lumen (Stirling et al., 1992; Stirling, C., unpublished results; Rose et al., 1989; Preuss et al., 1991; Sanders et al., 1992). Vesicles did not contain GDPase and α1->6 mannosyl-transferase activities; these enzymes reside in early compartments of the yeast Golgi complex and are part of the glycosylation machinery (Yanagisawa et al., 1990; Graham and Emr, 1991).

We demonstrate that vesicles purified from Yptlp-deficient reactions are vectorial transport intermediates on the basis of their ability to fuse with *cis*-Golgi membranes, but not with ER membranes. Diffusible ER-derived transport vesicles did not fuse with ER membranes under conditions that promote ER-membrane fusion (Fig. 6, *B* and *C*). Vesicle fusion with *cis*-Golgi membranes was detected only when purified vesicles were mixed with membranes and cytosol prepared from a wild-type strain. Fusion was efficient (20%) and required the addition of cytosolic protein, ATP, and incubation at physiologic temperature (Fig. 6, *C* and *D*). A mechanism that ensures the unidirectionality of vesicle movement is likely to be an integral component of transport vesicles. Perhaps the high concentration of Betl, Sec22, and Bosl proteins in vesicles relative to donor membranes prevents "back-fusion" with ER membranes, while promoting docking and fusion with *cis*-Golgi membranes. Alternatively, the absence of Kar2p in vesicles may ensure the directionality of fusion, since Kar2p-function is required for homotypic ER-membrane fusion (Latterich and Schekman, 1994).

Sorting of membrane and lumenal proteins precedes the scission of transport vesicles from ER membranes. This follows precisely because ER-derived vesicles contained only a subset of membrane and lumenal proteins that were initially mixed in the ER membrane (Fig. 2). We find that vesicles contain Betl, Sec22, and Bosl proteins, but not Sec61 and Kar2 proteins. The bulk flow hypothesis (Rothman, 1987) predicts that the absence of Sec61 and Kar2 proteins in vesicles is due to their active retention in the ER membrane. It will be interesting to determine if core-gpαf, Betlp, Sec22p, and Boslp are actively sorted into vesicles during budding. Quantitative electron microscopic analysis of immunostained "vesicle buds" on ER membranes should resolve this issue (Bednarek, S., L. Orci, and R. Schekman, unpublished results).

Electron microscopic analysis of thin sections that contained purified vesicles showed no apparent protein coats surrounding the vesicle membrane (Fig. 7, *C* and *D*). Nevertheless, subunits of coatomer were consistently detected on gradient-purified (see Table III and Fig. 10 *B*, lane *1*) and immunoisolated (Fig. 10 *B*, lanes *2*, *3*, and *5*) transport vesicles, but altogether constituted only 1% of the total vesicle protein; at this concentration coatomer is probably scattered on the vesicle surface. It is likely that ER-derived vesicles were initially coated with a protein lattice and lost the coat proteins during purification. High molecular weight proteins detected in immunoisolated transport vesicles, but not in gradient-purified vesicles, may represent components of such coats (Fig. 10 *A*, compare lane *6* to lanes *2*, *3*, and *5*); these are not subunits of coatomer because equivalent amounts of coatomer were detected in gradient-purified as well as in -immunoisolated transport vesicles (Fig. 10 *B*, compare lane *1* to lanes *2–4*). In other work we have shown that coatomer is not required in a reconstituted budding reaction. Instead, a distinct membrane coat formed by the Sec23/24 complex, the Sec13/31 complex, and Sarlp is found on ER-derived transport vesicles produced in the presence of nonhydrolyzable analogs of GTP (Barlowe et al., 1994). Interestingly, the gradient-purified transport vesicles described here are depleted of coat proteins (see Table III and Fig. 7), yet contain the information necessary to target and fuse with *cis*-Golgi membranes (Fig. 6 *D*); thus, it appears that coat proteins need not be maintained on vesicles to retain targeting competence.

The twelve most abundant proteins in purified ER-derived transport vesicles were tightly associated with the vesicle membrane and resisted extraction with 1 M potassium acetate or 0.2 M sodium carbonate at pH 11.5 (Fig. 8 *B*). These proteins were named ERV proteins. Two lines of evidence indicate that ERV proteins are components of ER-derived transport vesicles. First, the biochemical requirements for the release of membranes from perforated cells that contain ERV proteins were the same as for transport vesicles that contain radiolabeled core-gpαf (Fig. 11). Second, ERV proteins were abundant in immunoisolated transport vesicles, as well as gradient-purified vesicles (Fig. 10 *A*; compare lanes *2*, *3*, and *5* to lane *6*). None of the identified ERV proteins is Betl or Sec22 proteins since their absence in Triton X-100

eluates of immuno-beads (evidenced by Western blots; Fig. 10 *B*, compare lane *1* to lanes *2* and *5*) does not result in the absence of an ERV protein (evidenced by silver stain; Fig. 10 *A*, compare lane *6* to lanes *2*, *3*, and *5*). It remains to be determined whether ERV proteins and less abundant proteins in purified vesicle fractions (Fig. 8) play a functional role in vesicular transport, or are just cargo.

Three lines of evidence confirm the presence of core-gpαf, Betl, Sec22, and Bosl proteins in the same transport vesicles. First, the kinetics of release from perforated cells of membranes that contained Betlp, Sec22p, and core-gpαf were almost identical, as expected for proteins that reside in the same vesicle population (Fig. 2). Second, vesicles that were purified in gradients were highly enriched in all four proteins (Table III and Fig. 10 *B*, lane *1*). The fold enrichment of Betlp, Sec22p, and Boslp at each purification step was comparable. Nevertheless, vesicles that contain most of Sec22 and Bosl proteins were slightly denser (31% wt/wt) than the average Betlp and core-gpαf containing vesicle (30% wt/wt) in sucrose equilibrium density gradients (not shown). The small discrepancy in densities can best be explained by two possibilities; either these proteins are present in different types of ER-derived vesicles, or vesicles contain unequal amounts of all three proteins, which may influence vesicle density. To better determine whether proteins reside in the same vesicles or not, we used antibodies that recognize Betlp or Sec22p to immunoisolate ER-derived transport vesicles from MSS fractions with the premise that, if Betlp, Sec22p, Boslp, and core-gpαf reside in separate vesicles, they should not all be present in specific immunoisolates. Antibodies against Betlp, and antibodies against Sec22p, efficiently precipitated vesicles that contain all four proteins (Fig. 10, lanes *2*, *3*, and *5*); the relative ratio of these proteins with respect to each other was similar in vesicles purified in gradients or isolated in immuno-beads (Fig. 10 *B*; compare lane *1* with lanes *2*, *3*, and *5*). These results are in disagreement with those obtained by Lian et al. (1993) who reported that ER-derived transport vesicles lack detectable amounts of Betlp. This discrepancy may relate to the presence of functional Yptlp in their vesicle budding reaction. Perhaps Yptlp serves to regulate the packaging of certain vesicle membrane proteins and in its absence Betlp may be gathered into a bud. This role in protein segregation cannot be essential because vesicles purified from Ypt1-deficient reactions are competent to target and fuse with *cis*-Golgi membranes (Fig. 6, *C* and *D*) in a reaction that requires Yptlp-function (Rexach, M., unpublished results). In normal reactions, Ypt1 protein may become associated with transport vesicles during the budding reaction, however it is clear that this timing is not obligate and vesicles formed in the absence of Yptlp may acquire this protein in the course of targeting to the Golgi complex.

The finding that Betlp, Sec22p, Boslp, and coatomer are components of ER-derived transport vesicles, and the available genetic evidence on the various interactions between genes that encode these proteins (reviewed in Pryer et al., 1992), suggests a physical interaction between these proteins. We propose a model in which Sec22, Betl, and Bosl interact to form part of a docking complex that specifies and promotes the stable attachment of vesicles to *cis*-Golgi membranes. Coatomer may function to concentrate docking complexes in vesicles, or may mask active docking sites on the vesicle surface. Yptlp may monitor the subunit composition of docking complexes in ER-derived transport vesicles to promote vesicle attachment to *cis*-Golgi membranes.

The availability of functional ER-derived transport vesicles in highly purified form, combined with a cell-free assay that measures vesicle fusion with *cis*-Golgi membranes, will facilitate the further dissection of the mechanisms of vesicle targeting and membrane fusion. Because reconstituted vesicle fusion requires the addition of cytosolic factors, this provides a biochemical assay for the purification of soluble proteins that function at this stage. The generation of antibodies against surface constituents of transport vesicles should provide the tools necessary to examine the function of ERV proteins in reconstituted transport. The identification of genes that encode the ERV proteins should allow an assessment of their function in living cells.

The authors would like to thank all of the people who contributed with antibodies and technical advice. Special thanks to Drs. R. Ossig, C. Dascher, and D. Gallwitz who provided antibodies against Sec22p and Slylp, and to Y. Jiang and S. Ferro-Novick for alerting us the hexapeptide sequence shared by Boslp and Betlp. Thanks to Drs. S. Sanders, J. Thorner, M. Jaffe, T. Stevens, C. Slayman, N. Salama, C. Kaiser, D. Hosobuchi, T. Yoshihisa, R. Kahn, C. Barlowe, and S. Ferro-Novick, for antibodies against Sec61p, PGK, FlBo, VPM1, PM ATPase, Secl3p, Secl7p, coatomer, Sec23p, Arfp, Sarlp, and Boslp, respectively. We thank Susan Hamamoto for advice in electron microscopy, Bob Lesch for preparing radiolabeled ppαf, Dr. D. King for preparing peptides, and Drs. R. Duden and K. Wilson for comments on the manuscript.

This work was supported by grants form the National Institutes of Health and Howard Hughes Medical Research Institute to R. Schekman.

Received for publication 4 May 1994 and in revised form 15 June 1994.

References

Abeijon, C., and C. B. Hirschberg. 1992. Topography of glycosylation reactions in the endoplasmic reticulum. *Trends Biochem. Sci.* 17:32–36.

Baker, D., and R. Schekman. 1989. Reconstitution of protein transport using broken yeast spheroplasts. *Methods Cell Biol.* 31:127–141.

Baker, D., L. Hicke, M. Rexach, M. Schleyer, and R. Schekman. 1988. "Reconstitution of SEC gene product-dependent intercompartmental protein transport. *Cell.* 54:335–344.

Barlowe, C., C. d'Enfert, and R. Schekman. 1993*a*. Purification and characterization of Sar1p, a small GTP binding protein required for transport vesicle formation from the endoplasmic reticulum. *J. Biol. Chem.* 268:873–879.

Barlowe, C., and R. Schekman. 1993*b*. SEC12 encodes a guanine nucleotide exchange factor essential for transport vesicle budding from the ER. *Nature (Lond.).* 365:347–349.

Barlowe, C., L. Orci, T. Yeung, M. Hosobuchi, S. Hamamoto, N. Salama, M. Rexach, M. Ravazzola, and R. Schekman. 1994. COPII: a membrane coat formed by Sec proteins that drive vesicle budding from the ER. *Cell.* 77:895–907.

Becker, J., T.-J. Tan, H.-H. Trepte, and D. Gallwitz. 1991. Mutational analysis of the putative effector domain of the GTP-binding Ypt1 protein in yeast suggests specific regulation by a novel GAP activity. *EMBO (Eur. Mol. Biol. Organ.) J.* 10:785–792.

Brodsky, F. M. 1988. Living with clathrin: its role in intracellular membrane traffic. *Science (Wash. DC).* 242:1396–1402.

Clary, D. O., I. C. Griff, and J. E. Rothman. 1990. SNAPs, a family of NSF attachment proteins involved in intracellular membrane fusion in animals and yeast. *Cell.* 61:709–721.

d'Enfert, C., L. J. Wuestehube, T. Lila, and R. Schekman. 1991. Sec12p-dependent membrane binding of the small GTP-binding protein Sar1p promotes formation of transport vesicles from the ER. *J. Cell Biol.* 114:663–670.

Dascher, C., R. Ossig, D. Gallwitz, and H. D. Schmitt. 1991. Identification and structure of four yeast genes (SLY) that are able to suppress the functional loss of YPT1, a member of the RAS superfamily. *Mol. Cell Biol.* 11:872–885.

Esmon, B., P. C. Esmon, and R. Schekman. 1992. Early steps in the processing of yeast glycoproteins. *J. Biol. Chem.* 259:10322–10327.

Franzusoff, A., and R. Schekman. 1989. Functional compartments of the yeast Golgi apparatus are defined by the *sec7* mutation. *EMBO (Eur. Mol. Biol. Organ.) J.* 8:2695–2702.

Franzusoff, A., E. Lauzé, and K. E. Howell. 1992. Immunoisolation of Sec7p-coated transport vesicles from the yeast secretory pathway. *Nature (Lond.).* 355(Fig. 6356):173–175.

Graham, T. R., and S. D. Emr. 1991. Compartmental organization of Golgi specific protein modification and vacuolar protein sorting events defined in a yeast sec18 (NSF) mutant. *J. Biol. Chem.* 114(2):207–218.

Griff, I. C., R. W. Schekman, J. E. Rothman, and C. A. Kaiser. 1992. The yeast SEC17 gene product is functionally equivalent to mammalian αSNAP protein. *J. Biol. Chem.* 267(17):12106–12115.

Hardwick, K. G., and H. R. B. Pelham. 1992. SED5 encodes a 39-kD integral membrane protein required for vesicular transport between ER and the Golgi complex. *J. Cell Biol.* 119(3):513–521.

Harlow, E., and D. Lane. 1988. Antibodies: a laboratory manual. Cold Spring Harbor Laboratory, Cold Spring Harbor, N.Y.

Hicke, L., T. Yoshihisa, and R. Schekman. 1992. Sec23p and a novel 105kD protein function as a multimeric complex to promote vesicle budding from the ER. *Mol. Biol. Cell.* 3:667–676.

Hosobuchi, M., T. Kreis, and R. Schekman. 1992. SEC21 is a gene required for ER to Golgi protein transport that encodes a subunit of the yeast coatomer. *Nature (Lond.).* 360:603–605.

Jamieson, J., and H. Palade. 1967. Intracellular transport of secretory proteins in the pancreatic exocrine cell. I. Role of the peripheral elements of the Golgi complex. *J. Cell Biol.* 34:577–596.

Julius, D., R. Schekman, and J. Thorner. 1984. Glycosylation and processing of prepro-α-factor through the yeast secretory pathway. *Cell.* 36:309–318.

Kaiser, C., and R. Schekman. 1990. Distinct sets of SEC genes govern transport vesicle formation and fusion early in the secretory pathway. *Cell.* 61:723–733.

Keen, J. H. 1990. Clathrin and associated assembly and disassembly proteins. *Annu. Rev. Biochem.* 59:415–438.

Latterich, M., and R. Schekman. 1994. The karyogamy gene *KAR2* and novel proteins are required for ER membrane fusion. *Cell.* 78:87–98.

Lian, J. P., and S. Ferro-Novick. 1993. Bos1p, an integral membrane protein of the Endoplasmic reticulum to Golgi transport vesicles, is required for their fusion competence. *Cell.* 73:735–745.

Malhotra, V., T. Serafini, L. Orci, J. C. Sheperd, and J. E. Rothman. 1989. Purification of a novel class of coated vesicles mediating biosynthetic protein transport through the Golgi stack. *Cell.* 58:329–336.

Newman, A. P., M. Groesch, and S. Ferro-Novick. 1992. Bos1p, a membrane protein required for ER to Golgi transport in yeast, co-purifies with the carrier vesicles and with Bet1p and the ER membrane. *EMBO (Eur. Mol. Biol. Organ.) J.* 12:3609–3617.

Novick, P., C. Field, and R. Schekman. 1980. Identification of 23 complementation groups required for post-translational events in the yeast secretory pathway. *Cell.* 21:205–215.

Novick, P., S. Ferro, and R. Schekman. 1981. Order of events in the yeast secretory pathway. *Cell.* 25:461–469.

Oka, T., S. Nishikawa, and A. Nakano. 1991. Reconstitution of GTP-binding Sar1 protein function in ER to Golgi transport. *J. Cell Biol.* 114:671–679.

Orci, L., V. Malhotra, M. Amherdt, T. Serafini, and J. E. Rothman. 1989. Dissection of a single round of vesicular transport: sequential intermediates for intercisternal movement in the Golgi stack. *Cell.* 56:357–368.

Orci, L., D. J. Palmer, M. Amherdt, and J. E. Rothman. 1993. Coated vesicle assembly in the Golgi requires only coatomer and ARF proteins from the cytosol. *Nature (Lond.).* 364:732–734.

Palade, G. 1975. Intracellular aspects of the process of protein secretion. *Science (Wash. DC).* 189:347–358.

Palmer, D. J., J. B. Helms, C. J. Beckers, L. Orci, and J. E. Rothman. 1993. Binding of coatomer to Golgi membranes requires ADP-ribosylation factor. *J. Biol. Chem.* 268(16):12083–12089.

Pearse, B. M. F., and M. S. Robinson. 1990. Clathrin, adapters and sorting. *Annu. Rev. Cell Biol.* 6:151–171.

Preuss, D., J. Mulholland, C. A. Kaiser, P. Orlean, C. Albright, M. D. Rose, P. W. Robbins, and D. Botstein. 1991. Structure of the yeast endoplasmic reticulum: localization of ER proteins using immunofluorescence and immunoelectron microscopy. *Yeast.* 7(9):891–911.

Pryer, N., L. Wuestehube, and R. Schekman. 1992. Vesicle-mediated protein sorting. *Annu. Rev. Biochem.* 61:471–516.

Pryer, N. K., N. R. Salama, R. W. Schekman, and C. A. Kaiser. 1993. Yeast Sec13p is required in cytoplasmic form for ER to Golgi transport in vitro. *J. Cell Biol.* 120:867–875.

Rexach, M. R., and R. W. Schekman. 1991. Distinct biochemical requirements for the budding, targeting and fusion of ER-derived transport vesicles. *J. Cell Biol.* 114:219–229.

Rose, M. D., L. M. Misra, and J. P. Vogel. 1989. KAR2, a karyogamy gene, it is the yeast homologue of mammalian BiP/GRP78 gene. *Cell.* 57:1211–1221.

Roth, J., D. Brada, P. Lackie, J. Schweden, and E. Bause. 1990. Oligosaccharide trimming. Man_9 mannosidase is a resident ER protein and exhibits a more restricted and local distribution than glucosidase II. *Eur. J. Cell Biol.* 53:131–141.

Rothman, J. E. 1987. Protein sorting by selective retention in the endoplasmic reticulum and Golgi stack. *Cell.* 50:521–522.

Ruohola, H., A. Kastan Kabcenell, and S. Ferro-Novick. 1988. Reconstitution of protein transport from the endoplasmic reticulum to the Golgi complex in yeast: The acceptor Golgi compartment is defective in the sec23 mutant. *J. Cell Biol.* 107:1465–1476.

Salama, N. R., T. Yeung, and R. W. Schekman. 1993. The Sec13p complex and reconstitution of vesicle budding from the ER with purified cytosolic proteins. *EMBO (Eur. Mol. Biol. Organ.) J.* 12(11):4073–4082.

Sanders, S. L., K. M. Whitfield, J. P. Vogel, M. D. Rose, and R. W. Schekman. 1992. Sec61p and BiP directly facilitate polypeptide import into the ER. *Cell.* 69:353–365.

Schmitt, H., M. Puzicha, and D. Gallwitz. 1988. Study of a temperature-sensitive mutant of the ras-related *YPT1* gene product in yeast suggests a role in the regulation of intracellular calcium. *Cell.* 53:635–647.

Segev, N. 1991. Mediation of the attachment or fusion step in vesicular transport by the GTP-binding Ypt1 protein. *Science (Wash. DC).* 252:1553–1556.

Segev, N., J. Mulholland, and D. Botstein. 1988. The yeast GTP-binding Ypt1 protein and a mammalian counterpart are associated with the secretion machinery. *Cell.* 52:915–924.

Shim, J., A. Newman, and S. Ferro-Novick. 1991. The BOS1 gene encodes an essential 27 kD putative membrane protein that is required for vesicular transport from the ER to the Golgi complex in yeast. *J. Cell Biol.* 113:55–64.

Stamnes, M. A., and J. E. Rothman. 1993. The binding of AP1 clathrin adaptor particles to Golgi membranes requires ADP-ribosylation factor. *Cell.* 73(5):999–1005.

Stearns, T., R. A. Kahn, D. Botstein, and M. A. Hoyt. 1990. ADP ribosylation factor is an essential proteins in Saccharomyces cerevisiae and is encoded by two genes. *Mol. Cell. Biol.* 10:6690-6699.

Stearns, T., M. C. Willingham, D. Botstein, and R. A. Kahn. 1990. ADP-ribosylation factor is functionally and physically associated with the Golgi complex. *Proc. Natl. Acad. Sci. USA.* 87:1238–1242.

Stirling, C. J., J. Rothblatt, M. Hosobuchi, R. Deshaies, and R. Schekman. 1992. Protein translocation mutants defective in the insertion of integral membrane proteins into the endoplasmic reticulum. *Mol. Biol. Cell.* 3:129–142.

Südhof, T. C., and R. Jahn. 1991. Proteins of synaptic vesicles involved in exocytosis and membrane recycling. *Neuron.* 6:665–677.

Tsai, P.-K., L. Ballou, B. Esmon, R. Schekman, and C. Ballou. 1984. Isolation of glucose-containing high-mannose glycoprotein core-oligosaccharides. *Proc. Natl. Acad. Sci. USA.* 81:6340–6343.

Wagner, P., C. N. T. Molenaar, A. J. G. Rauh, R. Brokel, H. D. Schmitt, and D. Gallwitz. 1987. Biochemical properties of the ras-related YPT protein in yeast: a mutational analysis. *EMBO (Eur. Mol. Biol. Organ.) J.* 6(8):2373–2379.

Wuestehube, L. J., and R. Schekman. 1992. Reconstitution of transport from the endoplasmic reticulum to the Golgi complex using an ER-enriched membrane fraction from yeast. *Methods Enzymol.* 219:124–136.

Yanagisawa, K., D. Resnick, C. Abeijon, P. W. Robbins, and C. B. Hirschberg. 1990. A guanosine diphosphatase enriched in Golgi vesicles of Saccharomyces cerevisiae: purification and characterization. *J. Biol. Chem.* 265(31):19351–19355.

Yoshihisa, T., C. Barlowe, and R. Schekman. 1993. Requirement of a GTPase activating protein in vesicle budding from the endoplasmic reticulum. *Science (Wash. DC).* 259:1466–1468.